DISSERTATION

MECHANISMS OF VASCULAR DYSFUNCTION IN OBESITY AND TYPE 2 DIABETES: ROLE OF THE GUT MICROBIOTA AND ENDOPLASMIC RETICULUM STRESS

Submitted by

Micah Lee Battson

Department of Food Science and Human Nutrition

In partial fulfillment of the requirements

For the Degree of Doctor of Philosophy

Colorado State University

Fort Collins, Colorado

Spring 2018

Doctoral Committee:

Advisor: Christopher Gentile
Co-Advisor: Kimberly Cox-York

Tiffany Weir
Michael Pagliassotti
Adam Chicco

ABSTRACT

MECHANISMS OF VASCULAR DYSFUNCTION IN OBESITY AND TYPE 2 DIABETES: ROLE OF THE GUT MICROBIOTA AND ENDOPLASMIC RETICULUM STRESS

Vascular dysfunction, characterized by arterial stiffness and endothelial dysfunction, is a key antecedent to overt cardiovascular disease in obesity and type 2 diabetes. Although the mechanisms underlying the development of vascular dysfunction in obese and type 2 diabetic individuals are not fully known, a growing body of evidence suggest that adverse cellular processes, including endoplasmic reticulum (ER) stress, inflammation and oxidative stress, are primarily responsible for the disruption of normal vascular function in these two metabolic diseases. Therefore, identifying effective strategies to mitigate one or more of these adverse processes may lead to novel therapies for the treatment of vascular dysfunction in obesity and/or type 2 diabetes. In addition, ascertaining the initial triggering factor(s) that promote these adverse processes will inform innovative ways to prevent or control the progression of vascular dysfunction.

The goals of this dissertation research were to 1) examine the underlying causes of vascular dysfunction in obesity and type 2 diabetes and 2) identify potential strategies to mitigate vascular dysfunction in these metabolic diseases. To this end, we conducted three separate studies in murine models of obesity and/or type 2 diabetes aimed to modulate key factors that can affect vascular function. In all three studies, we measured aortic pulse wave velocity and endothelium-dependent dilation as clinically relevant indices of arterial stiffness and endothelial dysfunction, respectively. We also conducted various biochemical analyses to explore the potential mechanisms by which our experimental interventions altered vascular function.

In our first study (Chapter 2), we examined the role of ER stress in diabetic vascular dysfunction. In type 2 diabetic (*db/db*) mice, we found that chronic administration of the ER stress inhibitor, tauroursodeoxycholic acid (TUDCA), significantly reduced arterial stiffness and endothelial dysfunction. These vascular improvements were associated with reduced expression of ER stress-related genes within the aorta and surrounding perivascular adipose tissue (PVAT). Next (Chapter 3), we examined the role of the gut microbiota in the development of vascular dysfunction in obesity. We found that Western diet (WD)-induced obesity increased arterial stiffness, impaired endothelial function, and promoted endotoxemia-related inflammation. Antibiotic treatment to suppress the gut microbiota in WD-fed mice reduced arterial stiffness, improved endothelial function, and attenuated systemic and vascular inflammation. In our final study (Chapter 4), we examined whether gut dysbiosis represents a causal factor in the development of obesity-related vascular dysfunction. We found that transplant of gut microbiota from obese (*ob/ob*) to control mice promoted the development of arterial stiffness, and this was associated with reduced abundance of a symbiotic bacterium, *Akkermansia muciniphila,* decreased short-chain fatty acid levels, and increased gut permeability. In contrast, transplant of control microbiota to obese mice did not attenuate arterial stiffness.

Collectively, these studies in mice provided evidence that 1) mitigation of ER stress improves vascular function in type 2 diabetes, 2) gut dysbiosis contributes to vascular dysfunction in WD-induced obesity, and 3) an obese-type microbiota can promote arterial stiffening independent of body weight. Future clinical trials and mechanistic studies are needed to translate our findings to humans and to further examine the molecular mechanisms linking gut dysbiosis to vascular dysfunction.

DEDICATION

To my wife, Megan, and to my parents, Art and Kathy, for their endless support, encouragement, and love.

TABLE OF CONTENTS

ABSTRACT ii

DEDICATION iv

1. CHAPTER 1: INTRODUCTION 1

Obesity and Type 2 Diabetes Statistics and Risk of Cardiovascular Disease 1

Arterial Stiffness and Endothelial Dysfunction 2

Mediators of Vascular Dysfunction 4

Research Objectives 5

2. CHAPTER 2: TAUROURSODEOXYCHOLIC ACID REDUCES ARTERIAL STIFFNESS AND IMPROVES ENDOTHELIAL DYSFUNCTION IN TYPE 2 DIABETIC MICE 6

Summary 6

Introduction 7

Methods 8

Results 10

Discussion 11

Figures 14

Tables 17

3. CHAPTER 3: SUPPRESSION OF GUT DYSBIOSIS REVERSES WESTERN DIET-INDUCED VASCULAR DYSFUNCTION 18

Summary 18

Introduction 19

Methods 20

Results 26

Discussion 28

Figures 34
Tables 39
4. CHAPTER 4: OBESITY-RELATED ALTERATIONS IN THE GUT MICROBIOTA ELICIT ARTERIAL STIFFENING IN MICE 40
Summary 40
Introduction 41
Methods 42
Results 46
Discussion 49
Figures 53
Tables 58
5. CHAPTER 5: SUMMARY AND FUTURE DIRECTIONS 59
REFERENCES 61

CHAPTER 1: INTRODUCTION

Cardiovascular disease (CVD) remains the leading cause of death in the U.S. and worldwide despite remarkable advances in prevention and treatment. In 2015, 41.5 percent of the U.S. population had at least one subtype of CVD, such as hypertension, coronary artery disease, heart failure, or stroke. The most recent projections estimate that by 2035 nearly half of the U.S. population will have CVD with associated costs of over $1 trillion annually (55). The growing number of individuals with obesity and/or type 2 diabetes is recognized to be a major contributor to this rising tide of CVD. Therefore, elucidating the mechanisms that promote CVD in obesity and type 2 diabetes, and identifying potential therapeutic targets, is of paramount biomedical importance.

Obesity and Type 2 Diabetes Statistics and Risk of Cardiovascular Disease

The number of adults in the U.S. that are obese, defined as having a body mass index (BMI; kg/m^2) greater than 30, has risen dramatically in recent decades (93). Data from the National Health and Nutrition Examination Surveys (NHANES) estimates that the prevalence of obesity in the U.S. was 39.6 percent in 2015-16 (50), and this number is expected to increase in coming years (37). These statistics are particularly concerning because obesity is a major risk factor for CVD. In fact, obese individuals have about a 2-fold higher risk than normal weight individuals for coronary artery disease and stroke, and a 4-fold higher risk for heart failure (97). Much of this increased risk is explained by traditional CVD risk factors, including hypertension, dyslipidemia and type 2 diabetes.

The Centers for Disease Control and Prevention (CDC) reports that, as of 2015, nearly 30.3 million people in the U.S., or 9.4 percent of the population, have diabetes; and type 2 diabetes accounts for 90-95 percent of all diabetes cases (111). BMI is strongly and independently associated with increased risk of developing type 2 diabetes, and obese

individuals are 2.5-5 times more likely to be diagnosed with type 2 diabetes compared to those with normal BMI (43). The risk of developing CVD is about 2-4 times higher in people with type 2 diabetes compared with nondiabetics, and CVD represents the most common cause of death in this population (89). Although type 2 diabetes is often associated with other cardiovascular risk factors, the risk of CVD mortality remains two-fold higher in people with type 2 diabetes, even after adjusting for smoking, blood pressure, BMI, and total cholesterol (137).

The increase in CVD risk in obesity and type 2 diabetes is primarily attributable to the development of vascular dysfunction, which is characterized by stiffening of the large elastic arteries and endothelial dysfunction (25, 120, 132). Arterial stiffness and endothelial dysfunction commonly develop in obesity and type 2 diabetes before the onset of overt CVD, and are each independent risk factors for incident CVD (28, 92, 106). Arterial stiffness is a consequence of adverse structural and functional changes to the cells and extracellular matrix within the artery wall (57, 155). Decreased compliance of the large elastic arteries can profoundly affect systemic hemodynamics and cardiac function, contributing to CVD progression (42, 155). The endothelium performs many crucial functions, including the regulation of vascular tone and coagulation, and impairments in endothelial function is an initial step in the pathogenesis of atherosclerosis and other cardiovascular complications (9).

Arterial Stiffness and Endothelial Dysfunction

An important function of the large elastic arteries is to buffer the pulsatile nature of blood flow during each cardiac cycle. Due to the mechanical and functional properties of these arteries, they can expand to accommodate the large volume of blood ejected from the heart during systole and then recoil to propel that blood to more distal tissues during diastole. In doing so, they help minimize the difference between systolic and diastolic blood pressures (i.e. keep pulse pressure to a minimum). In certain disease states, however, these arteries can become less compliant (or stiffer) and lose their ability to perform this crucial function. Stiffening of the

large elastic arteries, such as the aorta, can be measured both clinically and in experimental animals by pulse wave velocity (PWV), and a high PWV is indicative of a stiffer, less compliant, artery. Individuals with obesity display a higher carotid-femoral PWV (cfPWV, a measure of central arterial stiffness) compared to normal weight individuals, and BMI is positively correlated with cfPWV (25). Arterial stiffness is also increased in people with type 2 diabetes (123, 132) and aortic PWV is a powerful independent predictor of mortality in this population (28).

Several mechanisms contribute to the development of arterial stiffening (103). While stiffening of smaller peripheral arteries is more dependent on vascular tone, aortic stiffness is mediated primarily by changes to extracellular proteins. In experimental animals, obesity and diabetes has been associated with increased aortic collagen deposition, decreased elastin (or increased elastin fragmentation), and increased formation of advanced glycation end-products (AGEs) – all of which contribute to increased aortic stiffening (25, 45, 46). These adverse changes are mediated in large part by a chronic increase in inflammation and oxidative stress, two hallmark features of obesity and diabetes (56).

The vascular endothelium is a single layer of cells that line the blood vessels that, in addition to serving as a barrier between the bloodstream and the surrounding tissues, perform many crucial functions relating to both vascular and systemic physiology (127). A healthy endothelium regulates normal changes in vascular tone (generally promoting vasodilation), inhibits coagulation, suppresses proliferation of vascular smooth muscle cells, and maintains an overall anti-inflammatory environment (105, 125). Endothelial dysfunction is a broad term that describes an imbalance in the normal functioning or homeostasis of the endothelium, and shifts the phenotype to a more coagulative, pro-inflammatory, pro-oxidative, vascoconstrictive phenotype (125). While any, or all, of these adverse phenotypic changes may be considered evidence of endothelial dysfunction, vascular reactivity is commonly used as a surrogate measure, whereby an impaired endothelium-dependent dilation (EDD; e.g. acetylcholine-mediated dilation) response is evidence of endothelial dysfunction.

As with arterial stiffness, inflammation and oxidative stress are the primary factors driving endothelial dysfunction in obesity and diabetes. For example, these two processes can impair endothelial function by reducing the bioavailability of endothelial-derived nitric oxide (NO), a potent vasodilatory molecule, and this can be observed as a reduction in EDD. Pro-inflammatory signaling can reduce NO bioavailability both directly through the suppression of NO production and indirectly through the promotion of oxidative stress. Endoplasmic reticulum (ER) stress has also recently emerged as a novel factor contributing to the development of vascular dysfunction.

The ER performs many crucial cellular functions, including protein folding, lipid biosynthesis, and calcium storage. When the normal balance between ER functional capacity and demand is disturbed, a state broadly termed ER stress, an adaptive signaling network is activated in order to restore ER homeostasis. This signaling network, called the unfolded protein response (UPR), is mediated by the activation of three ER transmembrane proteins: 1) double stranded RNA-dependent protein kinase-like ER kinase (PERK), 2) inositol-requiring ER-to-nucleus signaling protein 1 (IRE1), and 3) activating transcription factor 6 (ATF6) (29). Acute activation of these UPR transducers results in attenuation of global protein translation and activation of transcriptional networks that enhance ER functional capacity. However, chronic UPR activation, which can occur in diseases states such as obesity and type 2 diabetes, leads to cell dysfunction and death and may promote the development of vascular dysfunction either directly or via interactions with inflammation and oxidative stress (5, 27).

Mediators of Vascular Dysfunction

Chronic low-grade inflammation is a major factor contributing to the development of obesity- and diabetes-related vascular dysfunction (54, 112). Increased circulating and adipose tissue cytokines, such as interleukin-6 (IL-6), can induce vascular inflammatory signaling and oxidative stress, two key processes involved in the development of vascular dysfunction (9, 32). Although the cellular mechanisms involved in the progression of arterial stiffness and

endothelial dysfunction have received considerable attention, the initial source of this inflammation remains unknown. An emerging hypothesis for the origin of obesity-related inflammation is an elevation in circulating bacterial lipopolysaccharide (LPS or endotoxin). Indeed, a 2- to 3-fold increase in circulating LPS, termed "metabolic endotoxemia," has been observed in genetic obese (*ob/ob*) and high-fat diet (HFD) fed mice (15, 16). LPS can activate Toll-like receptor 4 (TLR4), a key mediator of innate immunity, to promote inflammation within the vasculature and systemically (67, 86). Of note, induction of ER stress downstream of TLR4 activation has been shown to contribute to endothelial dysfunction in high fat fed mice (68). Intriguingly, genetically diabetic (*db/db*) and HFD-fed mice with mutated TLR4 display preserved endothelial function (86). Collectively, these studies suggest that gut-derived inflammatory signals may represent a novel cause of vascular dysfunction in obesity and type 2 diabetes and provide the basis for further investigation.

Research Objectives

The goal of this dissertation was to examine the underlying causes of vascular dysfunction in obesity and type 2 diabetes. This was conducted using three separate, yet complementary, studies in which we assessed arterial stiffness and endothelial function in obese and/or diabetic mice following an experimental intervention. First, we treated type 2 diabetic (*db/db*) mice with tauroursodeoxycholic acid (TUDCA) to examine the contribution of ER stress (Chapter 2). Second, we treated Western diet-induced obese mice with broad-spectrum antibiotics to establish a role of the gut microbiota and link with endotoxemia (Chapter 3). Last, we used microbiota transplant between lean wild-type and obese leptin-deficient (*ob/ob*) mice to 1) determine whether adverse changes in the composition of the gut microbiota in obesity play a causal role in the development of vascular dysfunction and 2) test whether vascular dysfunction could be attenuated in obese mice by restoring a wild-type microbiota.

CHAPTER 2: TAUROURSODEOXYCHOLIC ACID REDUCES ARTERIAL STIFFNESS AND IMPROVES ENDOTHELIAL DYSFUNCTION IN TYPE 2 DIABETIC MICE[1]

Summary

Background/Aims: Endoplasmic reticulum (ER) stress has emerged as a potential mechanism contributing to diabetes and its co-morbidities. However, the importance of ER stress in diabetic vascular dysfunction is unclear. The purpose of the current study was to examine the effects of the ER stress inhibitor, tauroursodeoxycholic (TUDCA), on arterial stiffness and endothelial dysfunction in type 2 diabetic mice. Methods: Carotid and mesenteric artery endothelial function were assessed via ex vivo pressure myography and arterial stiffness was measured by aortic pulse wave velocity. The effects of TUDCA were examined both acutely (*ex vivo*) and chronically (250 mg/kg/day; i.p., 4 weeks). Results: Compared to C57BL/6J (CON) mice, db/db (DB) mice did not display carotid artery endothelial dysfunction; however, mesenteric artery endothelial function was markedly impaired. Acute incubation (*ex vivo*) and chronic administration (250 mg/kg/day; i.p.) of TUDCA improved endothelium-dependent dilation in DB mesenteric arteries, without affecting endothelium-independent dilation. Chronic TUDCA administration also reduced arterial stiffness and was associated with reductions in ER stress markers in the aortic and perivascular adipose tissue. Conclusions: These results suggest that ER stress may represent a novel cause of, and therapeutic target for, diabetic vascular dysfunction.

[1] This is the peer-reviewed but unedited manuscript version of the following article: Battson ML, Lee DM, Jarrell DK, Hou S, Ecton KE, Phan AB, Gentile CL. Tauroursodeoxycholic Acid Reduces Arterial Stiffness and Improves Endothelial Dysfunction in Type 2 Diabetic Mice. Journal of Vascular Research 2017: 54(5):280-287 (DOI: 10.1159/000479967). The final, published version is available at http://www.karger.com/?doi=10.1159/000479967.

Introduction

The epidemic of type 2 diabetes (T2D) continues to grow unabated, affecting over 25 million individuals in the US, with another 50 million classified as pre-diabetic (126). Among the numerous morbidities associated with T2D, cardiovascular disease (CVD) is the most common and critical. Individuals with T2D are more than twice as likely as non-diabetics to develop CVD during their lifetime; and CVD is the most common cause of death in diabetics, accounting for nearly 70% of diabetes-related fatalities (49, 89).

One of the key events that links T2D to CVD is the development of vascular dysfunction, and two components of vascular dysfunction, in particular, contribute to diabetes-related CVD: 1) arterial stiffness and 2) endothelial dysfunction. Both arterial stiffness and endothelial dysfunction precede clinical manifestations of CVD, and both are independent predictors of future cardiovascular events in type 2 diabetics (28, 148, 149). Therefore, considerable effort has been made to identify the underlying causes of diabetic arterial stiffness and endothelial dysfunction, but despite these efforts, the initiating events that lead to their development are still unclear.

The endoplasmic reticulum (ER) has recently emerged as an important regulator of metabolic processes. Dysfunction within the ER, broadly termed ER stress, evokes the unfolded protein response (UPR), an adaptive pathway that aims to restore ER homeostasis (20). Although the UPR is the first line of defense against ER stress, chronic activation of the UPR leads to cell dysfunction and death and has been implicated in the pathophysiology of cardio-metabolic diseases (44, 101). Therapies that mitigate ER stress, such as the chemical chaperone tauroursodeoxycholic acid (TUDCA), have been shown to alleviate several of these cardio-metabolic diseases associated with ER stress (102, 107). However, few studies have examined the role of ER stress in diabetic endothelial dysfunction (3, 60), and to our knowledge, no data are available regarding the effects of TUDCA on arterial stiffness. Therefore, the

purpose of the current study was to examine the effects of TUDCA administration on endothelial dysfunction and arterial stiffness in type 2 diabetic mice.

Methods

Animals and Experimental Design

Male control C57BL/6J mice and type 2 diabetic mice homozygous for a point mutation in the leptin receptor gene ($Lepr^{db}$) were obtained from the Jackson Laboratory (Bar Harbor, ME) at 16 weeks of age. Mice were acclimated for 2 weeks, and fed ad libitum purified diet (Teklad TD. 08113, 4% Corn Oil Diet, Envigo). Mice were housed in a temperature and humidity controlled environment on a 12h:12h light-dark cycle. All animal procedures were reviewed and approved by the Colorado State University Institutional Animal Care and Use Committee. Mice were divided into three groups: 1) control mice with no treatment (CON), 2) diabetic mice with no treatment (DB) and 3) diabetic mice that received tauroursodeoxycholic acid (DB+TUDCA) (EMD Millipore, Billerica, Massachusetts) via intraperitoneal injections at a dose of 250mg/kg/day for 4 weeks. Following the 4 week intervention, all mice were sacrificed at approximately 6 months of age.

Aortic Pulse Wave Velocity (aPWV)

Mice were anesthetized using 2% isoflurane and oxygen at 2L per minute, placed supine on a heating board with legs secured to ECG electrodes, and maintained at a target heart rate of ~450 bpm by adjusting isoflurane concentration. Doppler probes (20MHz) (Mouse Doppler data acquisition system; Indus Instruments) were placed on the transverse aortic arch and abdominal aorta and the distance between the probes was determined with precision calipers. Pre-ejection time, the time between the R-wave of the ECG and the foot of the Doppler signal, was determined for each site. aPWV was calculated by dividing the distance (cm) between the probes by the difference in pre-ejection times (seconds) of the thoracic and abdominal regions.

Animal Termination and Assessment of Vascular Endothelial Function

Mice were anaesthetized with isoflurane and euthanized by exsanguination via cardiac puncture. The aorta was excised and cleaned of surrounding perivascular adipose tissue (PVAT) on ice-cold physiologic saline solution (PSS: 0.288g NaH2PO4, 1.802g glucose, 0.44g sodium pyruvate, 20.0g BSA, 21.48g NaCl, 0.875g KCl, 0.7195g MgSO4 7H20, 13.9g MOPS sodium salt, and 0.185g EDTA per liter solution at pH 7.4) and flash frozen in liquid nitrogen for later analysis. Vascular function was determined as previously described (129). Briefly, carotid and second-order mesenteric arteries were excised in ice-cold PSS and placed in pressure myograph chambers (DMT Inc., Atlanta, GA) containing warm PSS, cannulated onto glass micropipettes and secured with suture. Arteries were equilibrated for 1 hour at 37°C and an intraluminal pressure of 50 mmHg. Arteries were constricted with increasing doses of phenylephrine (PE: 10^{-9} to 10^{-5} M) followed immediately by a dose-response with endothelium-dependent dilator acetylcholine (ACh: 10-9 to 10-4 M). After a washout period, a dose-response to endothelium-independent dilator sodium nitroprusside (SNP: 10^{-10} to 10^{-4} M) was obtained after pre-constriction to PE (10^{-5} M). For acute experiments, cannulated arteries were incubated with or without 0.5mM TUDCA for 1 hour prior to response curves. Percent dilation was calculated based on the maximal luminal diameter of each artery.

RNA Isolation, cDNA Synthesis, and Real-time PCR

Aortic and PVAT RNA was isolated with Trizol (Life Technologies, Grand Island, NY, USA) according to manufacturer's instructions. cDNA was synthesized using iScript (Bio-Rad, Hercules, CA, USA) from 0.25μg/μl RNA in a 20μl reaction. Primer sequences are shown in the Table 1. Samples were run in duplicate using an iCycler and iQ SYBR Green Supermix (Bio-Rad) with two-step amplification (95°C for 10s, followed by annealing at 60°C for 30s) for a total of 40 cycles. Expression patterns of genes of interest were normalized to constitutively expressed β2 microglobulin as the reference gene. Data were normalized by calculating the

ΔCq for each sample, which was derived by subtracting the Cq of the reference gene from the gene of interest. Relative quantitation ($\Delta\Delta$Cq) was derived by subtracting the ΔCq for the experimental sample from the average ΔCq of the control group. Fold change differences were calculated by $2^{-\Delta\Delta Cq}$.

Statistics

Data are expressed as mean ± SEM. Normality of data were confirmed via the Shapiro-Wilk test. Statistical analysis was performed using one-way ANOVA and Fisher's Least Significance Difference (LSD) post hoc test (SPSS for Windows, release 11.5.0; SPSS, Chicago, IL, USA). A p-value of <0.05 was considered statistically significant.

Results

Endothelial Function in Diabetic Mice and the Effects of Acute TUDCA Administration

We first examined dilatory responses in carotid arteries and found no differences between DB and CON mice in endothelium-dependent dilation (EDD; Figure 2.1A) or endothelium-independent dilation (EID; Figure 2.1B) in carotid arteries from CON and DB mice. Carotid artery diameter was also not affected by diabetic status (CON: 336.5 ± 5.4 vs DB: 333.1 ± 3.6 μm; $p > 0.05$). To examine regional differences in arterial endothelial function, we assessed EDD in second-order mesenteric arteries from CON and DB mice. EDD was markedly impaired in mesenteric arteries from DB compared to CON mice (Figure 2.2A and 2.2B). Pre-incubation for one hour with the ER stress inhibitor, TUDCA, significantly increased EDD in separate mesenteric arteries isolated from the same diabetic mice (DB+TUDCA) (Figure 2.2A and 2.2B). EID was not different between DB and DB+TUDCA arteries. The diameter of the mesenteric arteries were also not different between groups (CON: 156.8 ± 3.8 vs DB: 159.6 ± 7.0; $p > 0.05$).

Effects of Chronic TUDCA Administration on Arterial Stiffness and Mesenteric Endothelial Function

In light of the beneficial effects of acute TUDCA administration in isolated arteries, we next sought to determine the effects of chronic TUDCA administration (4 weeks, 250 mg/kg/day i.p.) on diabetic vascular dysfunction. Arterial stiffness, as measured by *in vivo* aortic pulse wave velocity (aPWV), was significantly greater in DB compared to CON, and was significantly reduced by chronic TUDCA administration in DB mice (Figure 2.3). The constrictive response to phenylephrine (PE) was not different between CON and DB mesenteric arteries, and was not altered by treatment with TUDCA (Figure 2.4A). Chronic TUDCA administration improved EDD in DB mice (Figure 2.4B). EID was also reduced in DB compared with CON mice, and was not affected by TUDCA (Figure 2.4C).

Effects of Chronic TUDCA Administration on ER Stress in Aortic and Perivascular Adipose Tissue

To provide insight into the mechanism by which TUDCA improved vascular function, the expression of ER stress-associated genes was measured in perivascular adipose tissue (PVAT) and the aorta. In the PVAT, DB mice displayed increased expression of CHOP and ATF4 (Figure 2.5C and 2.5D) and there was a trend for increased expression of spliced X-box binding protein (sXBP1; Figure 2.5B) compared to CON mice. Chronic TUDCA administration reduced PVAT expression of GRP78 and ATF4 (Figure 2.5A and 2.5D). In the aorta, DB mice tended to have increased expression of sXBP1 (Figure 2.5F) compared to CON, and TUDCA treatment significantly reduced GRP78 and sXBP1 (Figure 2.5E and 2.5F).

Discussion

ER stress has emerged as an important mediator of diabetes and its co-morbidities, although the role of ER stress in diabetic vascular dysfunction is largely unknown. Therefore,

the purpose of the current study was to examine the role of ER stress in diabetic arterial stiffness and endothelial dysfunction. We found that chronic administration of the ER stress inhibitor, TUDCA, in diabetic mice significantly reduced arterial stiffness, as determined by pulse wave velocity. Furthermore, acute and chronic TUDCA improved endothelium-dependent dilation in diabetic mice. These improvements were accompanied by a reduction of ER stress markers in the perivascular adipose tissue. Collectively, the results suggest that ER stress may be a therapeutic target for diabetes-related vascular dysfunction. The results also identify PVAT as a novel source of ER stress in diabetes. Lastly, the data provide novel information regarding the development of diabetic endothelial dysfunction along different regions of the vascular tree.

Over the last decade, ER stress has emerged as a novel mediator of metabolic disturbances in models of obesity and type 2 diabetes (52). More recent studies suggest that ER stress also mediates obesity-related and diabetic vascular dysfunction (3, 58, 60). Cheang et al., found that high fat diet-induced endothelial dysfunction and aortic ER stress were reversed by TUDCA administration (23). More recently, Choi and colleagues reported that TUDCA restored dilatory responses to acetylcholine in genetically diabetic mice (26). Results from the current study support and extend these findings in several ways. First, in addition to the beneficial effects of TUDCA on coronary artery endothelial function reported by Choi et al., we found that TUDCA improved endothelial function within the peripheral vasculature (i.e. mesenteric arteries). Second, in agreement with previous studies, we found that endothelium-independent dilation (via sodium nitroprusside) was impaired in DB mice (12, 85), suggesting broad vascular dysfunction in these mice in both the endothelium and underlying smooth muscle cells. Surprisingly, TUDCA did not affect EID responses, indicating that the protective effects of TUDCA are specific to endothelium-dependent dilation. Unfortunately, EID responses were not reported in the only other study examining the effects of TUDCA on vascular function in DB mice (26), and thus future studies are needed to corroborate the lack of an effect by

TUDCA. Third, we found that chronic TUDCA administration reduced arterial stiffness in DB mice. This is in agreement with other studies demonstrating an increase in PWV in DB mice compared to controls (64, 117), and to our knowledge, are the first data to demonstrate a protective effect of ER stress inhibition on arterial stiffness.

In the current study, EDD was dramatically impaired in the mesenteric arteries of diabetic mice (~80% reduction in max dilation), whereas no impairments were found in the carotid arteries. This finding of discrepant function along the arterial tree corroborates previous work from our laboratory and elsewhere suggesting that the mesenteric arteries are more susceptible than carotid arteries to metabolic disturbances (77, 144). The reasons for this differential susceptibility along the vascular tree are unclear, although one notable difference between mesenteric and carotid arteries is the lack of perivascular adipose tissue that accumulates along the carotid bodies, even in models of extreme obesity such as DB mice. This difference is particularly relevant given the increasing evidence that PVAT contributes to endothelial dysfunction and arterial stiffness in models of chronic disease (32, 38). The current data are the first to demonstrate that PVAT is a source of ER stress in diabetic mice, and the reduction of ER stress markers in PVAT following TUDCA treatment suggest that PVAT-ER stress may play a role in diabetes-related vascular dysfunction, although future studies are necessary to determine the causality of this relation.

It should be noted that neither acute nor chronic TUDCA treatment completely reversed vascular dysfunction in the current study. This may have been due to incomplete suppression of ER stress by TUDCA, which is supported by the partial decrease in ER stress markers in the aorta and PVAT. Alternatively, the finding may indicate that other factors, independent of ER stress, contribute to vascular impairments in DB mice. It is important to acknowledge that markers of ER stress in the present study were determined only at the gene level. Of the four UPR mediators examined, spliced XBP1 mRNA is the one mediator often determined at the

gene rather than protein level given that the removal of the 26 nucleotide intron results in XBP1 translation (51, 141). The lack of protein expression measurements in the remaining UPR markers is a noted limitation. Lastly, the db/db mice used in the current study is a commonly used strain for the study of type 2 diabetes. Still, the animal model is not without certain limitations in regards to the severity of metabolic dysfunction and the applicability to human disease (39, 87). In conclusion, we found that acute and chronic administration of TUDCA improved endothelium-dependent dilation and reduced arterial stiffness in diabetic mice. Although numerous questions remain unanswered, the results suggest that ER stress may represent a novel cause of, and therapeutic target for, diabetes-related vascular dysfunction.

Figures

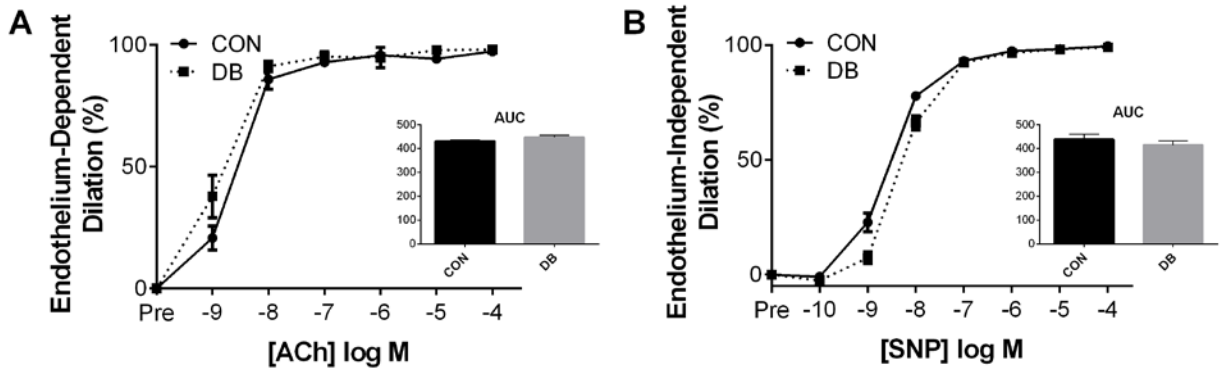

Figure 2.1. Carotid artery endothelial function is preserved in diabetic mice. Endothelium-dependent dilation (EDD) to acetylcholine (ACh) (A) and endothelium-independent dilation (EID) to sodium nitroprusside (SNP) (B) in control (CON; n = 6) and diabetic (DB; n = 7) carotid arteries.

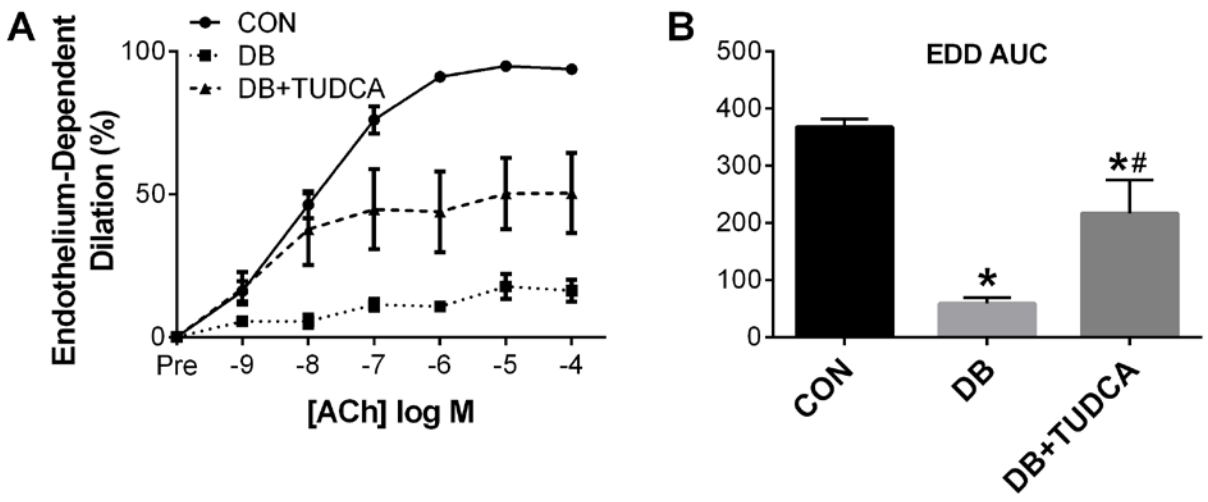

Figure 2.2. Mesenteric artery function is impaired in diabetic (DB) mice and is improved with acute incubation with TUDCA. Endothelium-dependent dilation (EDD) to acetylcholine (ACh) in control (CON) and DB mesenteric arteries pre-incubated with or without 0.5 mM TUDCA for 1 h (A). EDD expressed as AUC (B). * $p < 0.05$ vs. CON; # $p < 0.05$ vs. DB. CON: n = 12, DB: n = 6, DB + TUDCA: n = 6.

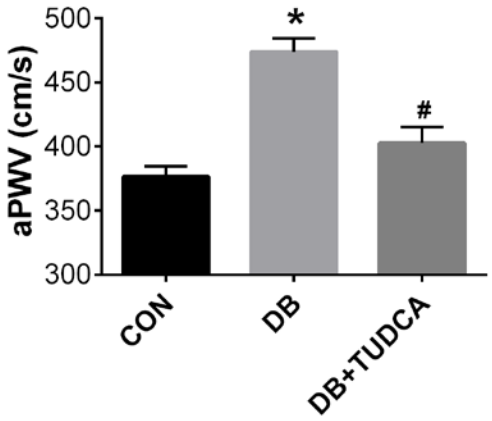

Figure 2.3. Chronic TUDCA administration reduces arterial stiffness in diabetic (DB) mice. Aortic pulse wave velocity (aPWV) in controls (CON), DB mice, and DB mice treated with TUDCA (DB + TUDCA; 250 mg/kg/day i.p. for 4 weeks). * $p < 0.001$ vs. CON; # $p < 0.001$ vs. DB. CON: n = 10, DB: n = 12, DB + TUDCA: n = 8.

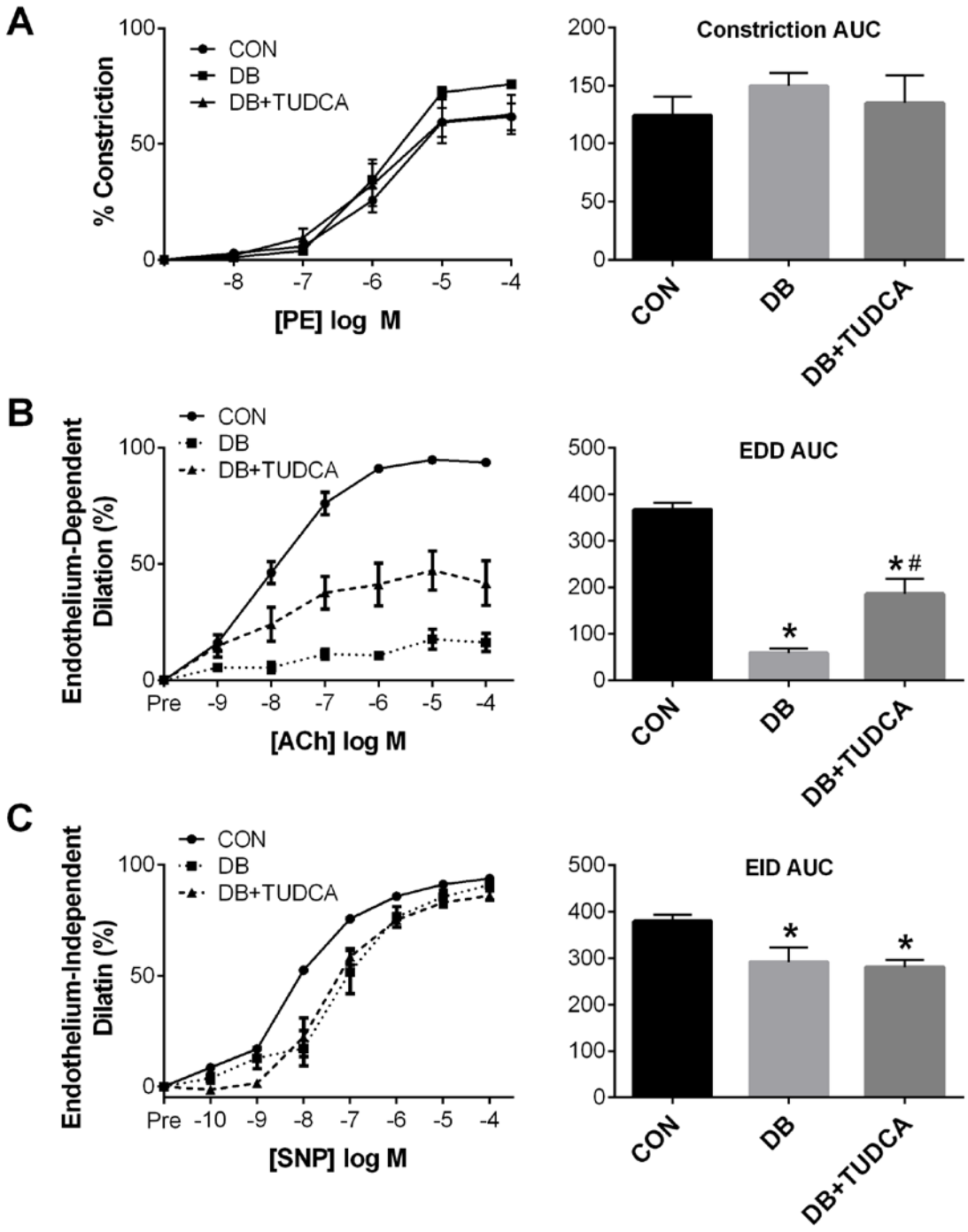

Figure 2.4. Chronic TUDCA administration improves mesenteric artery endothelial function in diabetic (DB) mice. Constriction to phenylephrine (PE) (A), endothelium-dependent dilation (EDD) to acetylcholine (ACh) (B), and endothelium-independent dilation (EID) to sodium nitroprusside (SNP) (C) in mesenteric arteries from controls (CON), DB mice, and DB mice treated with TUDCA (DB + TUDCA; 250 mg/kg/day i.p. for 4 weeks). * $p < 0.05$ vs. CON; # $p < 0.05$ vs. DB. CON: n = 12, DB: n = 6, DB + TUDCA: n = 6).

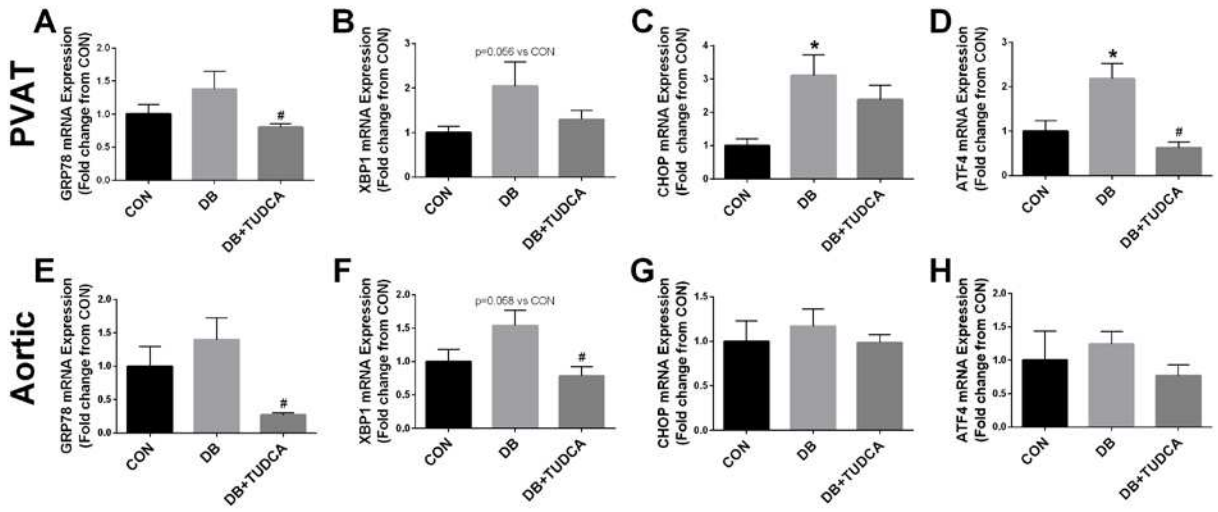

Figure 2.5. Chronic TUDCA administration reduces ER stress markers in the perivascular adipose tissue (PVAT) and aorta. Quantified mRNA expression in controls (CON), diabetic (DB) mice, and DB mice treated with TUDCA (DB + TUDCA; 250 mg/kg/day i.p. for 4 weeks). PVAT expression of GRP78 (A), sXBP1 (B), CHOP (C), and ATF4 (D). Aortic expression of GRP78 (E), sXBP1 (F), CHOP (G), and ATF4 (H). * $p < 0.05$ versus CON; # $p < 0.05$ versus DB. * $p < 0.05$ vs. CON; # $p < 0.05$ vs. DB. CON: n = 7–8, DB: n = 4–8, DB + TUDCA: n = 4–8 (sample numbers vary among genes examined).

Tables

Table 2.1. Sequence of qPCR primers for aortic and perivascular adipose tissue.

Target Gene	Sequence
B2M	(s) CGGTCGCTTCAGTCGTCAG
	(as) ATGTTCGGCTTCCCATTCTCC
CHOP	(s) CGCTCTCCAGATTCCAGTCAG
	(as) GTTCTCCTGCTCCTTCTCCTT
GRP78	(s) GAGGCGTATTTGGGAAAGAAGG
	(as) GCTGCTGTAGGCTCATTGATG
ATF4	(s) GAATGGATGACCTGGAAACC
	(as) GGCTCCTTATTAGTCTCTTGG
XBP1	(s) GGCATTCTGGACAAGTTGG
	(as) GAAAGGGAGGCTGGTAAGG

Note: β2 microglobulin (B2M), C/EBP homologous protein (CHOP), glucose-regulated protein 78 (GRP78), activating transcription factor 4 (AFT4), and X-box binding protein 1 (XBP1).

CHAPTER 3: SUPPRESSION OF GUT DYSBIOSIS REVERSES WESTERN DIET-INDUCED VASCULAR DYSFUNCTION[2]

Summary

Objective: Vascular dysfunction represents a critical pre-clinical step in the development of cardiovascular disease. We examined the role of the gut microbiota in the development of obesity-related vascular dysfunction. Approach and Results: Male C57BL/6J mice were fed either a standard diet (SD) (n=12) or western diet (WD) (n=24) for 5m, after which time, WD mice were randomized to receive either un-supplemented drinking water or water containing a broad-spectrum antibiotic cocktail (WD+Abx) (n=12/group) for 2m. Seven months of WD caused gut dysbiosis, increased arterial stiffness (SD: 412.0±6.0 vs WD: 458.3±9.0 cm/s, $p<0.05$) and endothelial dysfunction (28% decrease in max dilation, $p<0.05$), and reduced L-NAME-inhibited dilation. Vascular dysfunction was accompanied by significant increases in circulating LPS-binding protein (LBP) (SD: 5.26±.23 vs WD: 11±0.86 μg/mL, $p<0.05$) and interleukin-6 (IL-6) (SD: 3.27±0.25 vs WD: 7.09±1.07 pg/mL, $p<0.05$); aortic expression of phosphorylated nuclear factor-κB (p-NF-κB) ($p<0.05$); and perivascular adipose expression of NADPH oxidase subunit p67phox ($p<0.05$). Impairments in vascular function correlated with reductions in *Bifidobacterium spp*. Antibiotic treatment successfully abrogated the gut microbiota and reversed WD-induced arterial stiffness and endothelial dysfunction. These improvements were accompanied by significant reductions in LBP, IL-6, p-NF-κB, and advanced glycation end products (AGEs), and were independent from changes in body weight and glucose tolerance. Conclusions: These results indicate that gut dysbiosis contributes to the development of WD-

[2] This is the peer-reviewed but unedited manuscript version of the following article: Battson ML, Lee DM, Jarrell DK, Hou S, Ecton KE, Weir TL, Gentile CL. Suppression of Gut Dysbiosis Reverses Western Diet-Induced Vascular Dysfunction. Am J Phys Endo Metab. Epub 2017 Dec 26. (DOI: 10.1152/ajpendo.00187.2017). The final, published version is available at https://www.physiology.org/doi/10.1152/ajpendo.00187.2017

induced vascular dysfunction, and identify the gut microbiota as a novel therapeutic target for obesity-related vascular abnormalities.

Introduction

Intestinal microbes have emerged as critical regulators of human physiology (62). Disturbances to microbial equilibrium, broadly termed gut dysbiosis, have been linked to numerous disease processes (18). Diet is one of the most important determinants of microbial equilibrium, and dysbiosis that occurs secondary to a high fat or Western (high fat, high sugar) diet has been implicated in the pathogenesis of several diet-related diseases, including diabetes, steatohepatitis, and cardiovascular disease (CVD) (13).

Studies examining a link between the microbiota and CVD have focused primarily on hypertension and atherosclerosis (1, 33, 59, 91, 135, 154). However, numerous pre-clinical disturbances in the vasculature develop prior to overt atherosclerotic lesions. Among these disturbances, arterial stiffness and endothelial dysfunction are perhaps the most common and clinically relevant. Arterial stiffness and endothelial dysfunction are observed following Western diet feeding, and both are strong predictors of future cardiovascular events and mortality (28, 148). In light of this clinical importance, considerable attention has been given to identifying the cellular pathways that underlie the development of obesity-related arterial stiffness and endothelial dysfunction. In this regard, numerous studies in humans and experimental animals have shown that oxidative stress and inflammatory signaling are two critical mediators of vascular dysfunction (31, 40, 41, 70, 79, 108); although the initial source(s) of this oxidative stress and inflammatory signaling is still unclear.

Recent data indicate that gut dysbiosis may represent a novel source of oxidative stress and inflammation that could influence vascular function. For example, several microbial metabolites and structural bacterial components are capable of migrating from the intestinal environment and eliciting inflammation and oxidative stress within metabolically relevant tissues,

including the vasculature (15, 16, 71, 145). Despite these data, there is limited evidence to support a role of the gut microbiota in the development of endothelial dysfunction (22, 142), and to our knowledge, no data are available regarding the effects of dysbiosis on arterial stiffness. Therefore, the aim of the current study was to determine the effects of suppressing gut dysbiosis, via a broad-spectrum antibiotic cocktail, on arterial stiffness and endothelial dysfunction in Western diet-fed mice; and to examine potential factors that mediate gut-vascular crosstalk downstream of dysbiosis. Our results indicate that microbiota suppression improves both Western diet-induced arterial stiffness and endothelial dysfunction, and identify putative signals within the gut, the circulation, and the vasculature and perivascular adipose tissue that may mediate these vascular alterations.

Methods

Experimental Design

Male C57BL/6J mice were obtained from the Jackson Laboratory (Bar Harbor, ME) and acclimated for 2 weeks with *ad libitum* access to a standard diet (SD; TD.08113, Harlan Laboratories) consisting of 10.2% fat, 76.0% carbohydrate, and 13.8% protein calories. Mice were individually housed in a temperature- and humidity-controlled environment on a 12h:12h light-dark cycle. All animal procedures were reviewed and approved by the Colorado State University Institutional Animal Care and Use Committee. Once acclimated, 3-month-old mice were randomly assigned to a standard diet (SD; n=12) or Western diet (WD; n=24) (TD.88137, Harlan Laboratories) consisting of 42.0% fat (61.8% saturated, 27.3% monounsaturated, 4.7% polyunsaturated), 42.7% carbohydrate (80% sucrose), and 15.2% protein calories for 7 months. Body weight and food intake were recorded weekly. For the final 2 months of the dietary intervention (i.e. during months 5-7 on diet), WD mice were randomized to receive either non-supplemented drinking water (WD; n=12) or drinking water supplemented with a broad-spectrum antibiotic cocktail (WD+Abx; n=12) containing 0.4 g/L ampicillin (Cayman Chemical,

Ann Arbor, MI, #14417), 0.4 g/L neomycin sulfate (Cayman Chemical, Ann Arbor MI, #14287), 0.2 g/L vancomycin (Chem-Impex International, Wood Dale, IL, #00315), 0.4 g/L metronidazole (Research Products International, Mount Prospect, IL, #443-48-1) as described previously (47, 114). To avoid taste aversion-related reductions in fluid intake and weight loss commonly observed with antibiotic administration in mice (116), 1-5% glucose was added to the drinking water for all mice as advised by IACUC procedures for water additives.

Arterial Stiffness

Aortic pulse wave velocity (aPWV) was measured at 0, 3, 5 and 7 months on diet. Mice were anesthetized using 2% isoflurane and oxygen at 2L per minute, placed supine on a heating board with legs secured to ECG electrodes, and maintained at a target heart rate of ~450 bpm by adjusting isoflurane concentration. Doppler probes (20MHz) (Mouse Doppler data acquisition system; Indus Instruments, Houston, TX) were placed on the transverse aortic arch and abdominal aorta and the distance between the probes was determined simultaneously with precision calipers. Five consecutive 2-second recordings were obtained for each mouse and used to determine the time between the R-wave of the ECG and the foot of the Doppler signal for each probe site (Δtime). aPWV (in cm/s) was calculated as aPWV = (distance between the two probes) / ($\Delta time_{abdominal}$ - $\Delta time_{transverse}$).

Animal Termination and Tissue Collection

Mice were anaesthetized with isoflurane and euthanized by exsanguination via cardiac puncture. Blood was collected with an EDTA-coated syringe and immediately centrifuged at 1,000 rcf for 10min at 4°C to obtain plasma. Second-order mesenteric arteries were excised in ice-cold physiologic saline solution (PSS: 0.288g NaH2PO4, 1.802g glucose, 0.44g sodium pyruvate, 20.0g BSA, 21.48g NaCl, 0.875g KCl, 0.7195g MgSO4 7H20, 13.9g MOPS sodium salt, and 0.185g EDTA per liter solution at pH 7.4) and cannulated for vascular reactivity

experiments (see below). The thoracic aorta was excised and cleaned of surrounding perivascular adipose tissue (PVAT) on ice-cold PSS. A 1 mm segment of proximal aorta was frozen in optimal cutting temperature (OCT) media, transverse (7 µm) sections were obtained using a Microm HM550 cryostat (Thermo Scientific, Waltham, MA), and images were analyzed in CellSens imaging software (Olympus, Tokyo, Japan) for determination of morphological characteristics. The remainder of the aorta and PVAT were flash frozen and stored at -80°C for biochemical analyses. Cecum, and adipose tissue (subcutaneous, epididymal, and mesenteric depots) were isolated and weighed.

Vascular Reactivity

Endothelial function was determined via pressure myography. Second-order mesenteric arteries were placed in pressure myograph chambers (DMT Inc., Atlanta, GA) containing warm PSS, cannulated onto glass micropipettes and secured with suture. Arteries were equilibrated for 1 hour at 37°C and an intraluminal pressure of 50 mmHg. Arteries were constricted with increasing doses of phenylephrine (PE: 10^{-9} to 10^{-5} M) followed immediately by a dose-response with endothelium-dependent dilator acetylcholine (ACh: 10^{-9} to 10^{-4} M). Arteries were washed for 20 minutes and then incubated in the presence of the nitric oxide synthase inhibitor, L-N^{G}-Nitroarginine methyl ester (L-NAME, 0.1 mM, 30 minutes). With L-NAME present, a second dose-response to acetylcholine (ACh: 10^{-9} to 10^{-4} M) was performed following pre-constriction to PE (10^{-5} M) to determine the relative contribution of nitric oxide (NO) to endothelium-dependent dilation (EDD). After another 20 minute washout period, a dose-response to endothelium-independent dilator sodium nitroprusside (SNP: 10^{-10} to 10^{-4} M) was obtained after pre-constriction to PE (10^{-5} M). Artery diameters were measured by MyoView software (DMT Inc.) and used to calculate percent dilation for each dose of ACh or SNP relative to the PE-induced pre-constriction. Percent dilation (%) = (increase in luminal diameter to ACh/SNP) / (maximum decrease in luminal diameter to PE [10^{-5} M] pre-constriction) x 100. Area under the dose-

response curve (AUC; trapezoid method) was also calculated for each response. L-NAME-inhibited dilation was calculated as the percent reduction in maximal EDD in the absence vs. presence of L-NAME in each artery: L-NAME-inhibited dilation (% reduction in max EDD) = Max EDD_{ACh} - $EDD_{ACh\ w/\ L\text{-}NAME}$.

Microbiota Characterization

Fecal material was collected at termination and DNA extracted using the PureLink Microbiome DNA Purification Kit (A29790, Invitrogen, Carlsbad, CA). Quantitative PCR was used to verify suppression of the microbiota in Abx-treated animals. Reactions were optimized for the 16s rRNA gene using universal bacterial primers (forward: 5'-AAACTCAAAKGAATTGACGG-3', reverse: 5'-CTCACRRCACGAGCTGA-3') (4). Cycling conditions using the Biorad CFX96 thermal cycler were as follows: 95°C for 3min and then 40 cycles of 95°C 15s, 61°C 15s, 72°C 10s, 85°C 5s followed by florescence detection.

Paired-end sequencing libraries were constructed by following the Illumina 16s protocol which includes amplification of the V3-V4 regions of the 16s rRNA gene, purification of amplicons using AmPure beads, ligation with Illumina adaptors and dual indices, followed by another round of AmPure bead purification, quantification, denaturation and library pooling, and sequencing on an Illumina MiSeq. Paired fastq files were assembled and processed using the default myPhyloDB ver. 1.2.0 sequencing pipeline (90), which utilizes the mothur bioinformatics software for sequence processing (121). Briefly, sequences were screened (maxhomop=0, maxambig=1), chimeras removed, and classified to the K-mer based nearest neighbor (KNN) in the GreenGenes ver. 13_5 reference database. After processing, data were normalized by rarefaction based on a minimum sample size of 165,872 reads. Five hundred independent normalization runs were conducted and the average abundance for all normalization runs was used in further analyses.

Circulating Analytes

Plasma levels of insulin, leptin, and inflammatory cytokines interleukin-6 (IL-6), monocyte chemoattractant protein-1 (MCP-1) and plasminogen activator inhibitor-1 (PAI-1) were determined using a multiplex assay (MADKMAG-71K, EMD Millipore, Billerica, MA). Intra-assay variability (<5%) was within the normal limits reported by the manufacturer.

LPS-Binding Protein (LBP) and Soluble Cluster of Differentiation (CD)14

Due to well-established difficulties obtaining reliable circulating LPS levels, as well as limitations of commercially available chromogenic assays (10, 94), LPS signaling was determined by circulating levels of LBP and soluble CD14, two commonly used surrogates for LPS. Plasma LBP (ALX-850-304/1, Enzo Life Sciences,Farmingdale, NY) and soluble CD14 (#DC140, R&D Systems, Minneapolis, MN) were measured via ELISA per manufacturer's instructions using 1:800 and 1:40 dilution of plasma, respectively.

Aortic and PVAT Protein Expression

Aortas were homogenized using ZrO beads and a bullet blender (Next Advance, Averill Park, NY) in ice-cold RIPA lysis buffer containing protease and phosphatase inhibitors (Sigma, St. Louis, MO). Fifteen µg of aorta protein lysate was loaded on 4-12% gradient gels, separated by electrophoresis, and transferred to PVDF membranes for Western blot analysis. Blots were blocked with Odyssey Blocking Buffer TBS (LI-COR, Lincoln, NE) and incubated overnight at 4°C with primary antibodies against phospho-NF-kB p65 (1:500, #3033, Cell Signaling Technology [CST], Danvers, MA) and NF-kB p65 (1:500, #8242, CST). Perivascular adipose tissue (PVAT) was homogenized using the Minute™ Total Protein Extraction Kit for Adipose Tissues/Cultured Adipocytes (Invent Biotechnologies Inc., Plymouth, MN). As above, 30 µg of PVAT protein lysate was loaded for Western blot analysis with primary antibodies against p67 [phox] (1:500, BD Biosciences, San Jose, CA), NADPH oxidase 4 (NOX4, 1:1000, ab133303, abcam, Cambridge, MA) and advanced glycation end products (AGEs, 1:1000, ab23722,

abcam). Target proteins were detected using IRDye 680RD (1:15000, LI-COR), IRDye 800CW (1:15000, LI-COR) or IgG-HRP (1:5000, sc-2004, Santa Cruz Biotechnology, Dallas, TX) secondary antibodies and images were captured on Odyssey CLx (LI-COR) or EpiChemi^3 (UVP, Upland, CA)) imaging systems, respectively. Expression of each target protein was normalized to GAPDH (1:1000, #2118, CST), the ratio of phosphorylated/total protein calculated for each sample, and data is presented as fold change relative to SD.

Glucose Tolerance Test

At month 5 on diet and one week before experiment termination, mice were fasted for 6 hours and blood glucose was determined from tail vein blood using AlphaTRAK 2 glucose meters (Abbott Laboratories, Chicago, IL). Mice received an intraperitoneal injection of 2 g/kg dextrose and blood glucose was assessed at 0, 15, 30, 60, and 120 minutes post-injection.

Statistics

Data are expressed as mean ± SEM. Statistical analysis was performed using one-way ANOVA with Tukey's post hoc test (SPSS for Windows, release 11.5.0; SPSS, Chicago, IL). A mixed model ANOVA (within factor, time or dose; between factor, treatment group) was used for aPWV and EDD and EID dose response curves. When a significant main effect was observed, Tukey's post-hoc test was performed to determine specific pairwise differences. A p-value of <0.05 was considered statistically significant. Correlation analysis between outcome measures was performed using GraphPad Prism (La Jolla, CA).

Differential abundance of bacterial species was determined using the DESeq2 package in R and a False Discovery Rate of 0.05. Principle Component Analysis (PCA) was used to visualize separation of microbial communities between treatment groups. ANCoVA (significant; $p=0.01$) was used to determine differences in species abundance at the phyla level. Linear regression using Pearson's correlation and sparse Partial Least Square Regression analysis

(sPLS) were used to identify relationships between specific bacterial taxa and metavariables related to inflammation and vascular function outcomes.

Results

We first confirmed that antibiotic administration successfully abrogated intestinal microbes by qPCR using universal primers for the 16s ribosomal subunit. Bacterial count was similar between SD and WD mice, and significantly reduced with antibiotic treatment (WD+Abx) to levels observed in no template controls, confirming highly effective bacterial suppression (Figure 3.1A). Cecal mass was significantly reduced in WD and increased in WD+Abx (Figure 3.1B), as previously reported following high-fat feeding (152) and antibiotic treatment (48, 84, 95, 116, 119), respectively. In light of the marked microbial suppression with antibiotics, subsequent sequencing was not performed in antibiotic-treated mice.

Western diet resulted in marked alterations in the gut microbiota. For example, relative to SD, animals on a WD displayed significantly increased Firmicutes (SD=49,755; WD=109,454; p=0.0002), and decreased Bacteroidetes (SD=21,907; WD=11,205; p=0.016) and Actinobacteria (SD= 94.082; WD= 45,210; p= 0.003). PCA analysis showed sample clustering by diet type along PC1, with separation driven by *Ruminococcus gnavus* for WD and several *Bifidobacterium spp.* for SD (Figure 3.1C). Abundance of numerous bacterial taxa were altered by diet; in particular, *Bifidobacterium spp*. were significantly more abundant in SD animals compared to WD (Figure 3.1D).

Arterial stiffness progressively increased in WD mice during the 7 month intervention. In WD-fed mice that received antibiotic treatment (WD+Abx), arterial stiffness was completely normalized to SD levels (Figure 3.2A). Likewise, aortic media thickness was increased in WD compared to SD mice, and normalized in WD+Abx (Figure 3.2B). No group differences were observed for passive luminal diameter (SD: 161.7 ± 7.4, WD: 170.8 ± 6.7, WD+Abx: 174.9 ± 8.5 µm) or phenylephrine-induced pre-constriction (SD: 56.6 ± 5.5, WD: 59.0 ± 4.3, WD+Abx: 59.9 ±

4.4 %) in isolated mesenteric arteries. Similar to arterial stiffness, endothelium-dependent dilation (EDD) was significantly impaired in WD mice, and antibiotic treatment reversed this dysfunction (Figure 3.3A and 3.3B). Inhibition of nitric oxide synthase with L-NAME reduced EDD in all groups such that maximal acetylcholine-mediated dilation was similar in all groups (Figure 3.3C). L-NAME-inhibited dilation was reduced in WD mice, and restored with antibiotic treatment (Figure 3.3D). Endothelium-independent dilation was not altered by diet or antibiotic treatment (Figure 3.3E and 3.3F).

Body weight as well as epididymal and subcutaneous fat masses were significantly increased by WD, and unaffected by antibiotic treatment (Figure 3.4A-C). Plasma leptin and insulin levels were also elevated in WD and not significantly decreased by antibiotic treatment (Figure 3.4D-E). Likewise, WD significantly impaired glucose tolerance, with no effect of antibiotic treatment (Figure 3.4F).

To begin to explore potential mechanisms by which suppression of gut dysbiosis reversed vascular dysfunction, we assessed plasma levels of LPS-binding protein (LBP) and soluble cluster of differentiation-14 (sCD14), two markers of LPS signaling associated with cardiovascular outcomes (74). LBP (Figure 3.5A) and the LBP:sCD-14 ratio (Figure 3.5B) were increased in WD, and significantly reduced in WD+Abx. In light of these data, we next measured plasma levels of several pro-inflammatory mediators induced by LPS. IL-6 and PAI-1 were significantly increased in WD, but not WD+Abx; whereas MCP-1 was significantly decreased in WD+Abx (Figure 3.5C-E). To further examine potential mechanisms contributing to vascular dysfunction, we examined protein expression in the aorta and surrounding PVAT. Phosphorylation of NF-κB, which also occurs downstream of LPS signaling, was significantly increased in the aorta of WD mice, and normalized following antibiotic treatment (Figure 3.6A). PVAT expression of the p67phox, a regulatory subunit of NADPH oxidase (NOX) 2, was increased in WD, but not WD+Abx, compared to control-fed mice (Figure 3.6B). In contrast,

PVAT NOX4 expression was not different between groups (Figure 3.6C). Lastly, PVAT AGEs tended to be higher in WD (p=0.053 vs. SD), and were significantly decreased in WD+Abx compared to WD (Figure 3.6D).

Finally, we ran several correlation analyses to provide insight into the relations among alterations in bacterial species, inflammation, and vascular function. Several bacterial species were related to primary outcomes; in particular, three strains of *Bifidobacteria* were inversely correlated with body weight, LBP, and vascular function (Figure 3.7A and Table 3.1). Furthermore, LBP was significantly correlated with both indices of vascular function, L-NAME-inhibited dilation, and both systemic and vascular inflammation (Figure 3.7B-E). Collectively, these results lend support for a sequence of events wherein WD-induced reductions in B*ifidobacteria* increase LPS translocation and systemic signaling, which in turn propagates an inflammatory response that drives vascular dysfunction.

Discussion

The primary finding of the current study is that suppression of the microbiota via a broad-spectrum antibiotic cocktail reversed western diet-induced arterial stiffness and endothelial dysfunction. These vascular improvements were independent of changes in BW, fat mass and glucose tolerance; and were accompanied by reductions in LBP, markers of inflammation, and restoration of L-NAME-inhibited dilation. Lastly, the diet-induced vascular dysfunction correlated with reductions in several bacterial taxa, most notably several species of *Bifidobacterium*. Collectively, these results indicate that gut dysbiosis may be a causal factor in the development of vascular dysfunction, and suggest a potential role for bacterial-derived LPS in mediating these events. These results extend recent data linking gut dysbiosis to the development of other cardiovascular abnormalities, including atherosclerosis and hypertension (135), and lend further support to the notion that the gut microbiota represents a future therapeutic target for cardiovascular disease (69).

In the first study to examine a link between vascular function and gut dysbiosis, Vikram et al. elegantly demonstrated, using microbiota transplantations and antibiotic treatment, that gut dysbiosis can induce endothelial function via upregulation of vascular *miR-204* and subsequent downregulation of Sirt1 (142). The results of the present study complement and extend the findings by Vikram et al., in several ways. First, in addition to its effects on endothelial function, we found that suppression of the gut microbiota reversed WD-induced arterial stiffness, another clinically relevant feature of vascular function. Second, profiling of bacterial 16S ribosomal RNA revealed substantial dysbiosis in Western diet-fed mice, and identified changes in individual bacteria (e.g. reductions in *Bifidobacterium*) that are correlated with, and may drive, the observed vascular dysfunction. Third, Vikram et al. described a gut-vascular axis driven by increases in *miR-204* and subsequent reductions in Sirt1; and the authors note that they were unable to identify a circulating factor that governs crosstalk within this axis. Our data suggest that LPS signaling may represent one such circulating messenger. Indeed, LPS has been shown to increase m*iR-204*; LPS and *miR-204* have each been shown to decrease Sirt1 (63, 147); and Li et al., demonstrated that this m*iR-204*-Sirt1 axis is a critical mediator of LPS-induced inflammation (83). Thus, taken together, the two studies suggest that gut dysbiosis enhances LPS signaling in the general circulation, which in turn may impair vascular function via the miR-204-Sirt1 axis.

Chronic low-grade inflammation is a major factor contributing to the development of obesity-related vascular dysfunction (54). Increased circulating and adipose tissue cytokines, such as interleukin-6 (IL-6), can induce vascular inflammatory signaling and oxidative stress, two key processes involved in the development of vascular dysfunction (9, 32). An emerging hypothesis for the origin of obesity-related inflammation is an elevation in circulating bacterial lipopolysaccharide (LPS or endotoxin). Indeed, a 2- to 3-fold increase in circulating LPS, termed “metabolic endotoxemia,” has been observed in genetic obese (*ob/ob*) and high-fat diet (HFD)

fed mice (15, 16). Once in circulation, LPS elicits a potent inflammatory response at both systemic and local levels (15). To begin to explore putative mechanisms linking the gut dysbiosis to vascular dysfunction in the present study, we measured circulating levels of LBP and sCD14, two established surrogate measures of LPS independently associated with cardiovascular dysfunction (74). Although LBP and sCD14 expression are both stimulated by LPS, sCD14 is reported to have suppressing effects on endotoxin. In support of this notion, increased sCD14 has been associated with lower levels of the pro-inflammatory cytokine IL-6 in both plasma and adipose tissue despite higher plasma endotoxemia (75). Thus, an elevated LBP:sCD14 in plasma may be used as a surrogate marker of endotoxemia. In line with this, LBP and LBP:sCD14 ratio was significantly increased in mice fed a Western diet and reduced following antibiotic treatment. These results are in agreement with Li et al., who reported that enhanced LPS translocation subsequent to gut dysbiosis mediated atherogenesis in apoE$^{-/-}$ mice fed a Western diet (82).

Mechanistically, LPS can activate Toll-like receptor 4 (TLR4), a key mediator of innate immunity, to promote inflammation within the vasculature and systemically (67, 86). Downstream of TLR4, the transcription factor nuclear factor-κB (NF-κB) can promote vascular inflammation through upregulation of pro-inflammatory cytokines, adhesion molecules and pro-oxidant enzymes such as NADPH oxidase (11). We found that antibiotic treatment reduced circulating levels of IL-6 and MCP-1, and vascular phosphorylation of NF-κB, all of which are regulated by LPS and are established mediators of vascular dysfunction (133). In addition, NF-κB activation can suppress the expression of endothelial nitric oxide synthase (eNOS), a key enzyme that regulates vascular homeostasis through the production of the vasodilatory and anti-inflammatory molecule nitric oxide (NO) (78). Although eNOS expression or phosphorylation was not directly measured in the current study, our finding that dilation following L-NAME inhibition, a measure of NO-dependent dilation, was reduced by WD feeding and

restored with antibiotic treatment suggests that altered NO bioavailability may have contributed to the observed differences in vascular function. However, it should be noted that L-NAME-inhibited dilation is not equivalent to NO bioavailability and L-NAME may affect the oxidative status in the vasculature independent of its effects on NO. Thus, future studies are needed to more comprehensively determine the role of NO in mediating vascular alterations in the setting of gut dysbiosis.

A growing body of evidence suggests that changes to the perivascular adipose tissue can strongly influence vascular structure and function (53, 66, 99, 143). For example, studies by Fleenor and colleagues have found that accumulation of advanced glycation end products (AGEs) in aortic PVAT contributes to arterial stiffening with aging (38, 100). In the present study, we found that PVAT accumulation of AGEs tended to be higher in WD-fed mice ($p=0.053$) compared to control mice, and were significantly reduced with antibiotic treatment. Importantly, AGEs can increase oxidative stress, at least in part through activation of the pro-oxidant NADPH oxidase enzymes (46, 146). In line with this, we observed that WD-fed mice, but not antibiotic-treated mice, displayed increased PVAT expression of the NADPH oxidase 2 (NOX2) subunit p67phox. As previously observed, an increased expression of NOX2 and p67phox within PVAT may contribute to oxidative stress in obese mice (66, 150). Because NOX2 activity is influenced by multiple regulatory subunits (130), additional studies are needed to confirm whether these observed effects on p67phox protein expression are directly related to a rise in oxidative stress in the vasculature and PVAT. Interestingly, we found that PVAT expression of constitutively active NOX4 was not altered by WD feeding or antibiotic treatment. Together, these data suggest that dysbiosis is associated with increased NOX2, but not NOX4, within the PVAT. Western diet feeding also induced aortic remodeling, as evidenced by an increase in aortic media thickness, which was abrogated by antibiotic treatment. These data are the first to confirm that alterations in the gut microbiota can influence PVAT, and collectively suggest a

sequence of events whereby a Western diet induces gut dysbiosis and LPS translocation to the general circulation, eliciting an inflammatory response in the vasculature and PVAT that ultimately results in arterial stiffness and endothelial dysfunction. In a recent review, Xia and colleagues described the “obesity triad” wherein inflammation, hypoxia, and oxidative stress initiate a deleterious cycle within the PVAT that culminates in the development of vascular dysfunction (151). Although LPS signaling was not an element of the signaling cascade originally described by the authors, and PVAT inflammation does not require a hypothetical transfer of circulating or endothelial material, it is possible that LPS signaling may exacerbate the obesity triad and facilitate vascular dysfunction. Future studies utilizing genetic ablation of LPS signaling (e.g. CD14) and downstream mediators (e.g. IL-6, NF-κB, NADPH oxidase) are necessary to more definitively test this hypothesis and determine the specific signaling cascades involved.

Rodent models of Western diet-induced obesity display similar phylum-level changes to their microbial composition as those observed in obese individuals, including an increased Firmicutes:Bacteroidetes ratio (80, 138), and these changes have been associated with metabolic perturbations (16). Suppression of the gut microbiota with antibiotics has been used in numerous animal models to establish a causal role of the gut microbiota in disease risk or progression (21, 76, 113, 136). For example, antibiotics were used to establish an obligate role of the gut microbiota in the production of the pro-atherogenic compound trimethylamine *N*-oxide (TMAO) (145).

Although antibiotics have been widely used as an experimental tool to examine the effects of microbiota suppression on host physiology, the approach is not without limitations. First, although the antibiotics used in the current study successfully eliminated the gut bacteria and are poorly absorbed (72, 73, 115), we cannot say with absolute certainty that their actions were exclusively localized to the intestine and without systemic effects. Second, the broad-

spectrum antibiotic cocktail used in the current study suppresses all gut bacteria, even those which have been shown to positively modulate cardiovascular function, such as *Akkermansia muciniphila* (82). Thus, this approach precludes us from determining the specific microbial alterations that mediate the observed vascular protection. However, some insight was gained regarding the bacterial changes that mediate Western diet-induced vascular dysfunction. We observed significant decreases in several *Bifidobacterium spp*. following WD that correlated with both vascular dysfunction and inflammatory parameters. These results are in agreement with those from Cani et. al., who reported that enhancing *Bifidobacterium* populations improved glucose tolerance and reduced inflammation in diet-induced diabetic mice (17). More recently, a study by Catry et al., reversed endothelial dysfunction in apoE$^{-/-}$ mice fed an n-3 polyunsaturated fatty acid-depleted diet through supplementation of inulin-type fructans (ITFs) (22). Of note, the improvement in endothelial function with ITF-supplementation was accompanied by a dramatic increase in abundance of cecal *Bifidobacterium.*

We acknowledge that the lack of an additional control group fed a standard diet (SD) and receiving antibiotics is a significant limitation of the present study. Previous research has not observed an effect of antibiotic treatment in control low-fat diet-fed mice on markers of endotoxemia or metabolic parameters (16, 21). Given that SD-fed mice displayed normal vascular function, we did not anticipate that inclusion of a SD + Abx group would provide any significant insight regarding the role of gut dysbiosis in mediating vascular dysfunction. However, we did observe a slight age-related increase in aPWV in our SD group. Thus, if this increase was related to changes in microbial composition, then antibiotic treatment may have attenuated this increase. Regardless of this limitation, our results demonstrate that Western diet-induced dysbiosis represents an important factor in the development of vascular dysfunction.

In conclusion, the present work corroborates previous research linking gut dysbiosis to endothelial dysfunction, and is the first to demonstrate that suppression of gut dysbiosis reverses Western diet-induced arterial stiffness. The data also provide mechanistic insight into the downstream mediators of this dysfunction, and lend further support for the development of microbiota-targeted therapies in the treatment and prevention of cardiovascular disease.

Figures

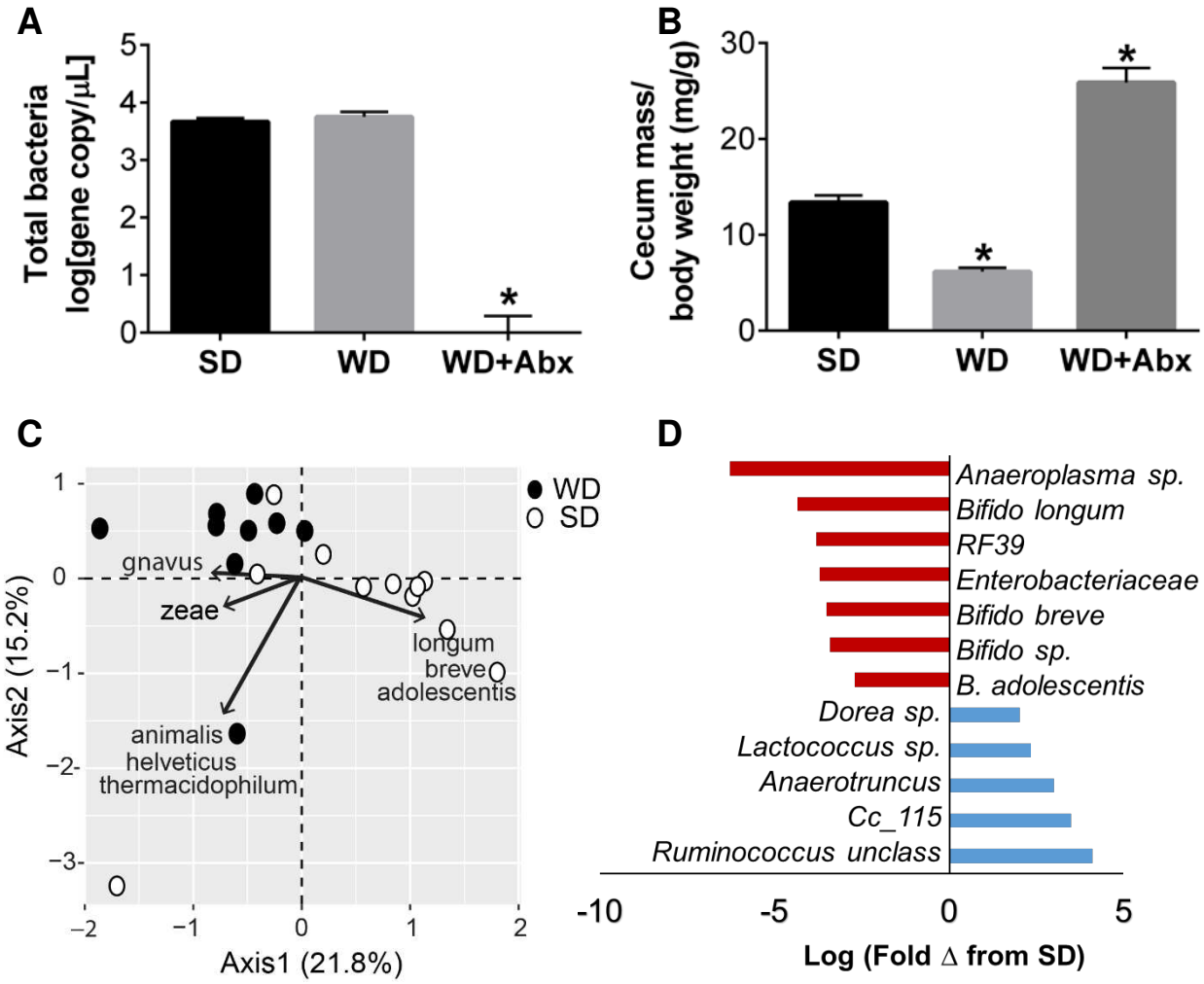

Figure 3.1. Antibiotic treatment suppresses the gut microbiota following Western diet-induced dysbiosis. Changes in total bacteria count following standard diet (SD), Western diet (WD) and WD with antibiotic (Abx) treatment (A); Cecal mass following WD and antibiotic treatment (B); PCA biplot of mouse fecal microbial communities colored by diet (closed circles=WD; open circles=SD) and indicating bacterial species driving variability in each quadrant (C); Histogram of significantly differentially abundant bacterial taxa in WD relative to

SD (q=0.05) represented as log fold-change (D). Statistical analysis was performed using one-way ANOVA with Tukey's post hoc test. Data are expressed as mean ± SEM; n = 10-12/group. *P < 0.05 vs all other groups.

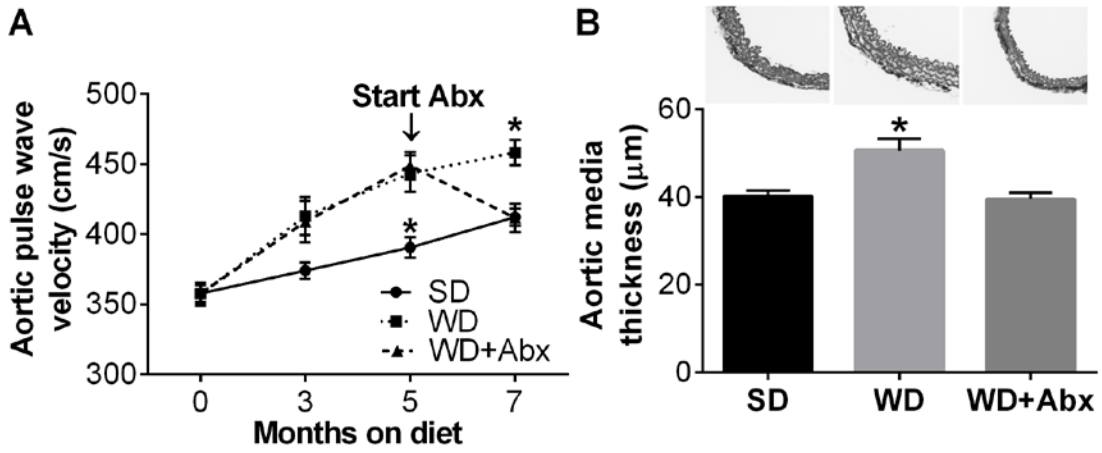

Figure 3.2. Antibiotics reverse Western diet-induced arterial stiffness. Arterial stiffness was serially measured by *in vivo a*ortic pulse wave velocity (aPWV) (A). Antibiotic treatment in a subset of WD mice was initiated following 5 months of WD feeding as indicated. Media thickness was determined in segments of proximal thoracic aorta (B). Statistical analysis was performed using repeated-measures ANOVA (aPWV) and one-way ANOVA (media thickness) with Tukey's post hoc test. Data are expressed as mean ± SEM; n = 10-12/group. *P < 0.05 vs all other groups.

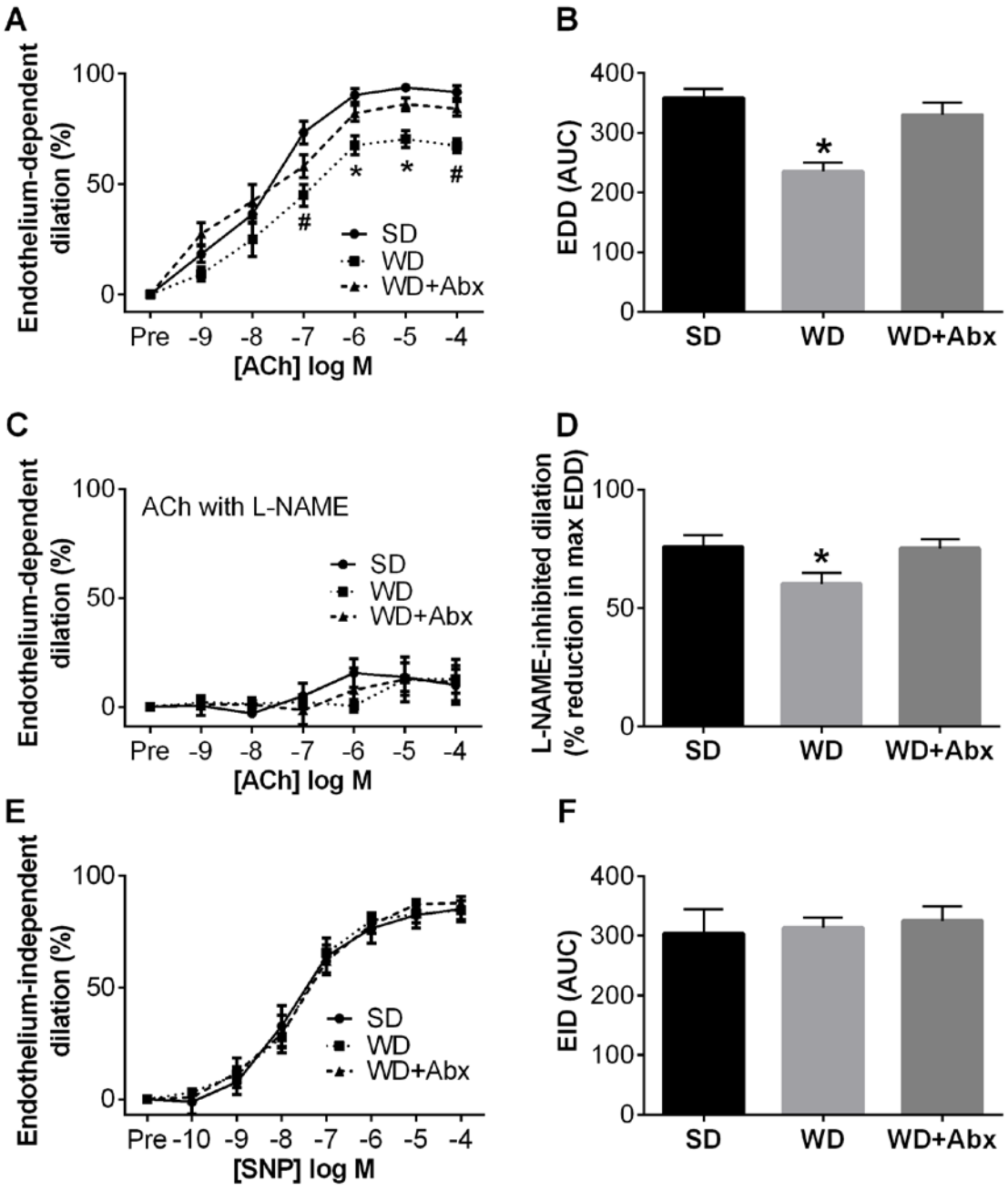

Figure 3.3. Antibiotics reverse Western diet-induced endothelial dysfunction and restore L-NAME-inhibited dilation. Endothelium-dependent dilation (EDD) to acetylcholine (ACh) alone (A-B) and in the presence of nitric oxide synthase inhibitor, L-NAME (C) was determined in mesenteric arteries. L-NAME-inhibited dilation, a measure of NO-dependent dilation, was calculated as the percent reduction in maximal EDD in the absence vs presence of L-NAME (D). Endothelium-dependent dilation (EID) to sodium nitroprusside (SNP) (E-F). Statistical analysis was performed using a repeated-measures ANOVA (EDD and EID dose responses) and one-way ANOVA (all other outcomes). When a significant main effect was observed, Tukey's post-hoc test was performed to determine specific pairwise differences. Data are expressed as mean ± SEM; n = 8-12/group. *P < 0.05 vs all other groups, #P < 0.05 vs SD.

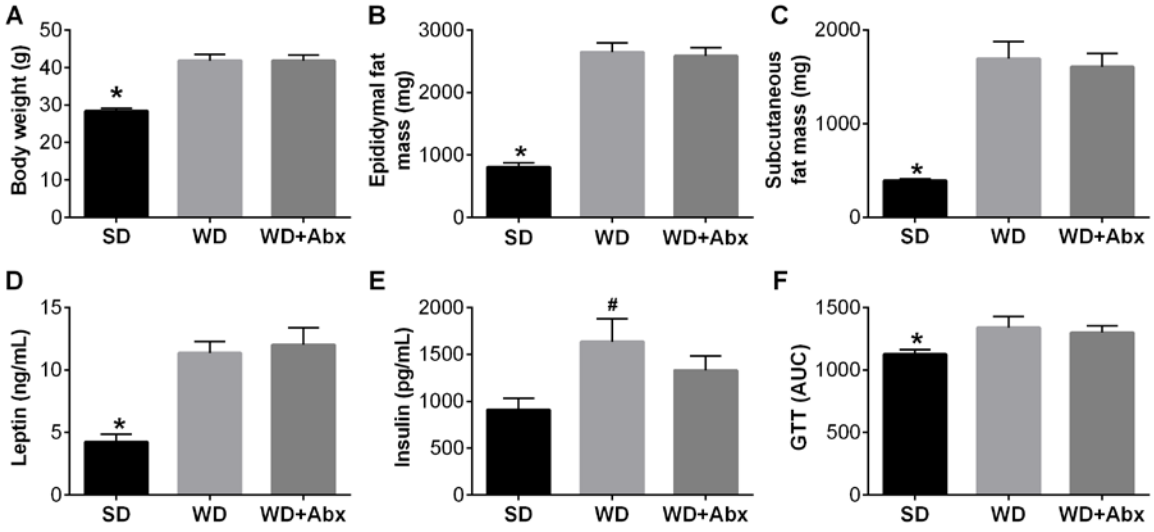

Figure 3.4. Antibiotic treatment does not alter body composition or glucose tolerance. Body weight (A), epididymal fat mass (B), subcutaneous fat mass (C) following WD feeding and antibiotic treatment. Plasma leptin (D) and insulin (E) were determined via multiplex ELISA. Area under the curve (AUC) for i.p. glucose tolerance test (GTT) (F). Statistical analysis was performed using one-way ANOVA with Tukey's post hoc test. Data are expressed as mean ± SEM; n = 10-12/group. *P < 0.05 vs all other groups.

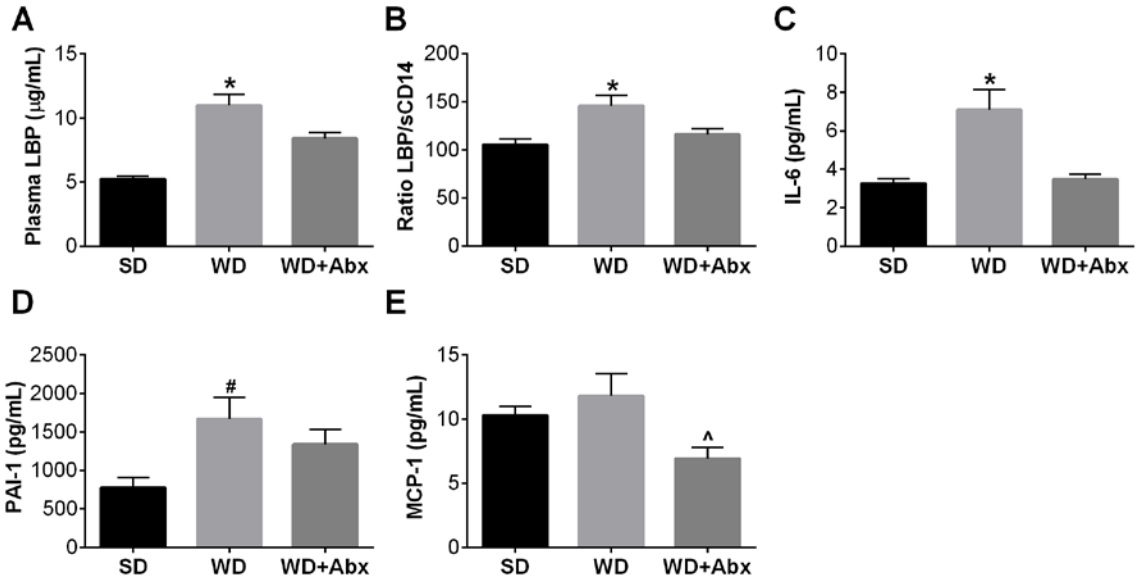

Figure 3.5. Antibiotic treatment attenuates Western diet-induced increases in circulating markers of endotoxemia and inflammation. Circulating LBP (A); LBP/sCD14 (B); IL-6 (C), PAI-1 (D) and MCP-1 (E) were determined in plasma via ELISA. Statistical analysis was performed using one-way ANOVA with Tukey's post hoc test. Data are expressed as mean ± SEM; n = 5-12/group. *P < 0.05 vs all other groups, #P < 0.05 vs SD, ^P < 0.05 vs WD.

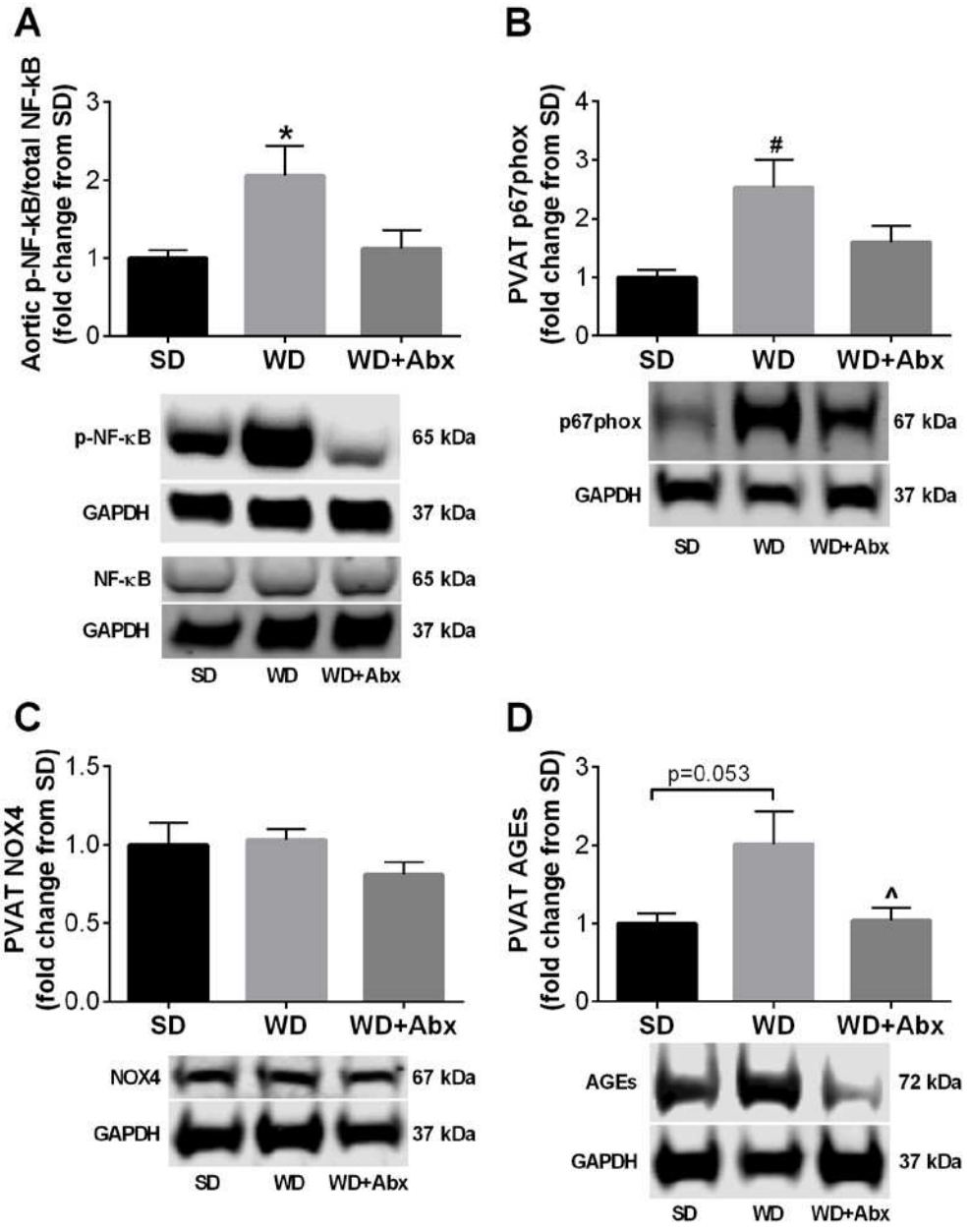

Figure 3.6. Antibiotic treatment attenuates Western diet-induced increases in proteins related to inflammation and oxidative stress. The ratio of phosphorylated to total NF-κB was determined in aorta via western blotting (A). Abundance of NADPH oxidase (NOX) 2 subunit p67phox (B), NOX4 (C) and advanced glycation end products (AGEs) (D) were determined in perivascular adipose tissue (PVAT) via western blotting. GAPDH expression was used to account for protein loading differences. Representative blots are shown below each graph. Statistical analysis was performed using one-way ANOVA with Tukey's post hoc test. Data are expressed as mean ± SEM; n = 7-12/group. *P < 0.05 vs all other groups, #P < 0.05 vs SD, ^P < 0.05 vs WD.

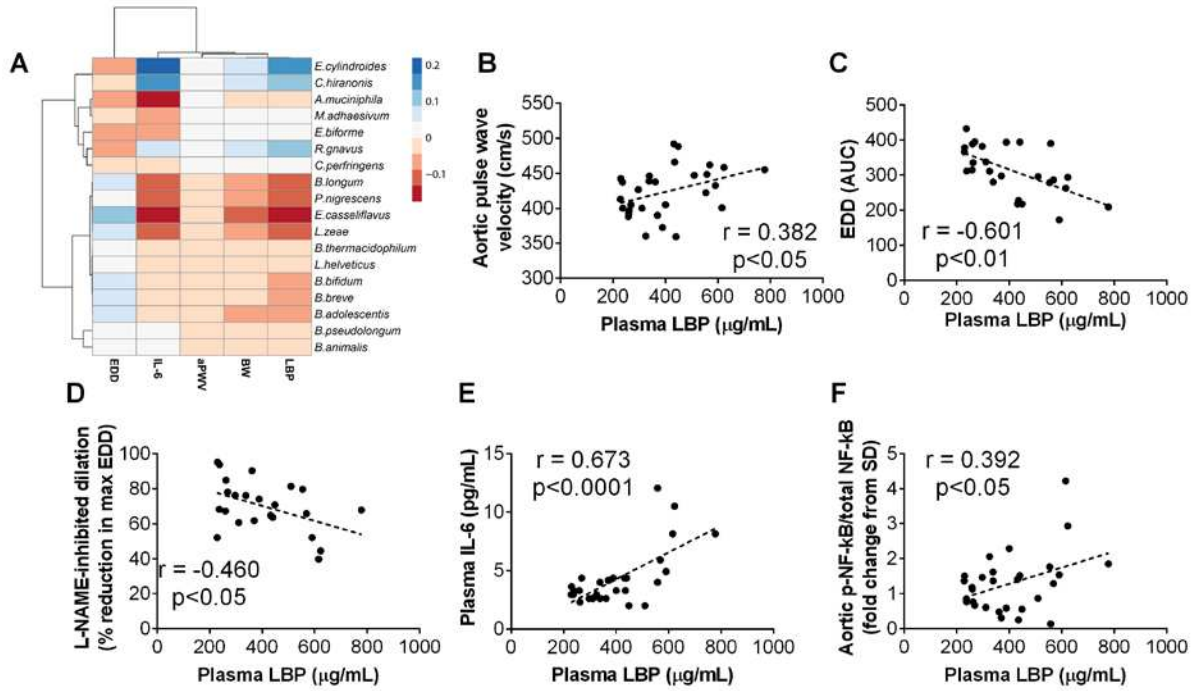

Figure 3.7. Correlation of bacterial abundance and LBP with vascular function and inflammatory markers. Heat map indicating correlations between bacterial species and specific outcome measures, including LPS binding protein (LBP), body weight (BW), aortic pulse wave velocity (aPWV), interleukin-6 (IL-6) and endothelium-dependent dilation (EDD) (A). Correlation of plasma LBP with aPWV (B), EDD (C), L-NAME-inhibited dilation (D), plasma IL-6 (E), and aortic p-NF-κB (F). Pearson correlation coefficient (r) and p values are indicated in figure; n = 7-12/group.

Tables

Table 3.1. Correlations between bacterial abundances and physiological outcomes in standard and Western diet-fed mice.

	B. breve	*B. longum*	*B.adolescentis*	*Allo-baculum*	*Lacto-coccus*	*Dorea*
EDD	r=0.55*	r=0.49*	r=0.52*	r=-0.62*	r=-0.49*	r=-0.66*
aPWV	r=-0.42	r=-0.6*	r=-0.63*	r=0.43*	r=0.27	r=0.51*
LBP	r=-0.50*	r=-0.57*	r=-051*	r=0.61*	r=0.61*	r=0.7*
BW	r=-0.55*	r=-0.58*	r=-0.51*	r=0.66*	r=0.60*	r=0.69*

Note: Mixed data from SD and WD groups were used for correlations. *B.*= Bifidobacterium; EDD = endothelium-dependent dilation; aPWV = aortic pulse wave velocity; LBP = LPS binding protein; BW = body weight. n = 9-12/group; *=p<0.05

CHAPTER 4: OBESITY-RELATED ALTERATIONS IN THE GUT MICROBIOTA ELICIT ARTERIAL STIFFENING IN MICE

Summary

Objective: To determine whether adverse changes in the composition of the gut microbiota in obesity play a causal role in the development of vascular dysfunction and test if vascular dysfunction can be attenuated in obese mice by restoring a control-type microbiota. Approach and Results: Following suppression of endogenous microbiota by 2 weeks antibiotic treatment, pooled donor cecal contents from leptin-deficient *ob/ob* (Ob) mice were transplanted by oral gavage for 8 weeks to wild-type (Con) mice, and vice versa. Control transplants from homologous donors were also performed. All mice (n=9-11/group) were given ad libitum access to a purified maintenance diet for the duration of the study. Arterial stiffness was measured by aortic pulse wave velocity and endothelial function was determined via pressure myography in isolated mesenteric arteries. Cecal short-chain fatty acids (SCFAs) were quantified by LC/MS and intestinal barrier function was determined via FITC-dextran gut permeability assay. Transplant of the Ob microbiota to Con mice significantly reduced the abundance of *Akkermansia muciniphila* and cecal concentration of SCFAs, and increased gut permeability (79% increase vs Con+Con, $p<0.05$) and arterial stiffness (Con+Ob: 415.3 ± 5.5 vs Con+Con: 385.6 ± 6.7 cm/s, $p<0.05$). Transplant of the Con microbiota to Ob mice increased SCFAs, but did not alter gut permeability (2% decrease vs Ob+Con, $p>0.05$) or arterial stiffness (Ob+Con: 485.3 ± 6.4 vs Ob+Ob: 492.9 ± 5.3 cm/s, $p>0.05$). Endothelial function and weight gain were not affected by microbiota transplant in either Con or Ob mice. Conclusions: These results demonstrate that the gut microbiota of Ob mice can contribute to the development of arterial stiffness, independent of weight gain. However, transplant of a Con microbiota was not able to attenuate vascular dysfunction in Ob mice.

Introduction

Obese individuals are at an elevated risk for cardiovascular diseases (CVD) due in large part to the development of vascular dysfunction (131, 132). Currently, more than one third of adults in the United States are considered obese, with that number predicted to increase to 42% by 2050 (55). Given the current demographic trends, obesity-related CVD has the potential to be an enormous biomedical and societal burden. Therefore, identifying the mechanisms that contribute to the development of vascular dysfunction in obesity is of high biomedical importance.

Vascular dysfunction is characterized by arterial stiffness and endothelial dysfunction, two strong independent risk factors of future CVD and mortality (92, 106). Chronic low-grade inflammation in obesity plays a major role in the pathogenesis of vascular dysfunction (112). Inflammatory signaling within the vascular wall as well as elevations in circulating pro-inflammatory cytokines are strongly linked to maladaptive structural changes to arteries and impaired endothelial homeostasis; however, the factor(s) initiating this obesity-related inflammation and vascular dysfunction are not fully known.

Translocation of microbial components from the gut, including bacterial endotoxins, has been implicated in the origin of obesity-related inflammation and may represent a link between obesity and elevated cardiovascular risk (15, 98). This increased absorption of gut-derived inflammatory stimuli can result from gut barrier disruption. In fact, studies in experimental animals demonstrate that impairment of the gut barrier and elevation of circulating bacterial components is associated with the development of insulin resistance and atherosclerosis (15, 16, 82).

The gut microbiota represents a key factor regulating gut barrier function, and obesity-related changes to the gut microbiota, termed dysbiosis, have been shown to alter intestinal homeostasis (35). For example, reductions in *Akkermansia muciniphila*, a symbiotic mucin-

degrading bacterium in the phyla Verrucomicrobia, are related to increased gut permeability, endotoxemia and inflammation in rodent models of cardiometabolic disease (19, 35, 82). Reduced abundance of *A. muciniphila* are observed in rodent models of genetic (*ob/ob*) (34-36) and diet-induced obesity (122); and *A. muciniphila* levels in humans are lower in overweight/obesity and inversely correlated with weight gain (61, 118). On the other hand, augmenting the abundance of *A. muciniphila* through either direct probiotic supplementation or treatment with prebiotic fibers has been shown to reduce endotoxemia and related inflammation (36, 82).

Collectively, these previous studies support the hypothesis that an increase in gut permeability, secondary to gut dysbiosis, may enhance pro-inflammatory signaling and thereby contribute to the development of obesity-related vascular dysfunction. Indeed, recently published work in rodent models have provided evidence of a direct link between gut dysbiosis and both arterial stiffness (7) and endothelial dysfunction (7, 59, 142). However, none of these studies investigated the association between increased gut permeability and the development of vascular dysfunction in obesity. Therefore, the aim of this study was to test the hypotheses that 1) the altered composition of the gut microbiota of leptin-deficient *ob/ob* (Ob) mice contribute to the development of vascular dysfunction and 2) the gut microbiota of wild-type (Con) mice can attenuate vascular dysfunction in Ob mice.

Methods

Experimental Design

All animal procedures were reviewed and approved by the Colorado State University Institutional Animal Care and Use Committee. Male leptin-deficient mice homozygous for the obese spontaneous mutation, Lep^{ob} (Ob), and wild-type C57BL/6J (Con) mice were obtained from The Jackson Laboratory (Bar Harbor, ME) and acclimated for 2 weeks in a temperature- and humidity-controlled environment on a 12h:12h light-dark cycle. Mice were housed in pairs

with *ad libitum* access to a purified maintenance diet (TD.08485, Envigo Teklad Diets, Madison, WI) consisting of 13.0% fat, 67.9% carbohydrate, and 19.1% protein calories for the duration of the study.

Donor cecal material was collected from a subset of Ob and Con mice (n=6/group) following confirmation of the presence and absence of vascular dysfunction, respectively. Pooled Ob and Con donor material was diluted 1:20 in sterile PBS, aliquoted and stored at -80°C until needed. To suppress the endogenous microbiota, Con and Ob recipient mice were given a broad-spectrum antibiotic cocktail (consisting of vancomycin [5mg/mL, Chem-Impex International, Wood Dale, IL, #00315], neomycin sulfate [10 mg/mL, Cayman Chemical, Ann Arbor MI, #14287], metronidazole [10 mg/mL, Research Products International, Mount Prospect, IL, #443-48-1] and ampicillin [10 mg/mL, Cayman Chemical, Ann Arbor, MI, #14417] via daily oral gavage (10 mL/kg) as well as ampicillin (1 g/L) supplemented to the drinking water for 2 weeks. This depletion protocol has been used effectively to suppress the gut microbiota in mice and avoids the issue of taste aversion-related weight loss when this same cocktail is given via drinking water (Reikvam 2011). Ampicillin, which has broad-spectrum activity but does not produce taste aversion, was added the drinking water to ensure a continuous antibiotic exposure to the gut microbiota. Following microbial suppression, Con and Ob recipient mice were randomized to receive donor cecal material via serial oral gavage (100 µL once daily for 5 days, followed by bi-weekly booster inoculations) to re-colonize their gut microbiota, resulting in four groups: Con+Con (n=9), Con+Ob (n=11), Ob+Con (n=10), and Ob+Ob (n=10). Body weight and food intake were recorded weekly during the transplant period.

Arterial Stiffness

Aortic pulse wave velocity (aPWV) was measured as previously described (6, 7). Briefly, mice were anaesthetized with isoflurane and placed supine on a heating board with legs secured to ECG electrodes. Doppler probes (20MHz) were placed on the transverse aortic arch

and abdominal aorta and the distance between the probes was determined simultaneously with precision calipers. Five consecutive 2-second recordings were obtained for each mouse and used to determine the time between the R-wave of the ECG and the foot of the Doppler signal for each probe site (Δtime). aPWV (in cm/s) was calculated as aPWV = (distance between the two probes) / ($\Delta time_{abdominal}$ - $\Delta time_{transverse}$).

Gut Permeability

Mice were water-fasted for 12 hours over night prior to oral gavage of 600mg/mL FITC-dextran (4,000 mol. wt.) diluted in PBS. After four hours, during which time food was also withheld, blood was collected via tail bleed for determination of plasma FITC-dextran concentration. Plasma samples were diluted 1:2 in PBS and fluorescence was measured on a spectrophotometrer at 485/20 (Excitation) and 528/20 (Emission). Concentrations were calculated based on a standard curve of known FITC-dextran concentrations prepared in control plasma from untreated mice and reported in µg/mL.

Animal Termination and Tissue Collection

Mice were anaesthetized with pentobarbital and euthanized by exsanguination via the pulmonary artery. Blood was collected with a syringe and immediately centrifuged at 2,000 rcf for 10min at 4°C to obtain serum. Second-order mesenteric arteries were excised in ice-cold physiologic saline solution (PSS) and cannulated for vascular reactivity experiments (see below). The spleen, cecum and adipose tissue depots (subcutaneous, epididymal, and mesenteric) were isolated and weighed. Colon length was recorded, then 2 mm segments of distal ileum and proximal colon were either frozen directly in optimal cutting temperature (OCT) media or fixed for 24 hours in Periodate-Lysine-Paraformaldehyde (PLP) buffer and embedded in paraffin wax. The thoracic aorta was excised and cleaned of surrounding perivascular

adipose tissue (PVAT) on ice-cold PSS. The aorta, PVAT and cecal contents were flash frozen and stored at -80°C for biochemical analyses.

Vascular Reactivity

Endothelial function was determined via pressure myography as previously described (6, 7). Briefly, second-order mesenteric arteries were placed in pressure myograph chambers (DMT Inc., Atlanta, GA) containing warm PSS, cannulated onto glass micropipettes and secured with suture. Arteries were equilibrated for 1 hour at 37°C and an intraluminal pressure of 50 mmHg. Arteries were constricted with increasing doses of phenylephrine (PE: 10^{-9} to 10^{-5} M) followed immediately by a dose-response with endothelium-dependent dilator acetylcholine (ACh: 10^{-9} to 10^{-4} M). Arteries were washed for 20 minutes and then a dose-response to endothelium-independent dilator sodium nitroprusside (SNP: 10^{-10} to 10^{-4} M) was obtained after pre-constriction to PE (10^{-5} M). Artery diameters were measured by MyoView software (DMT Inc.) and used to calculate percent dilation for each dose of ACh or SNP relative to the PE-induced pre-constriction. Percent dilation (%) = (increase in luminal diameter to ACh/SNP) / (maximum decrease in luminal diameter to PE [10^{-5} M] pre-constriction) x 100. Area under the dose-response curve (AUC; trapezoid method) was also calculated for each response.

Microbiota Characterization

Fecal material was collected at termination and DNA extracted using the PureLink Microbiome DNA Purification Kit (A29790, Invitrogen, Carlsbad, CA). Paired-end sequencing libraries were constructed by following the Earth Microbiome protocol (http://press.igsb.anl.gov/earthmicrobiome/protocols-and-standards/16s/), which includes amplification of the V4 regions of the 16s rRNA gene, purification of amplicons using AmPure beads, quantification, denaturation and library pooling, and sequencing on an Illumina MiSeq. Paired-end sequence reads were concatenated and all combined 16s sequences were filtered,

trimmed and processed with the DADA2 (R bioconductor package47) implementation included in the open source bioinformatics tool myPhyloDB version 1.2.1 (www.myphylodb.org/). Briefly, all primers were removed from each sequence using the open source Python program Cutadapt48 and sequence variants were inferred using the default pipeline in DADA2. Each sequence variant identified in DADA2 was classified to the closest reference sequence contained in the Green Genes reference database (Vers. 13_5_99) using the usearch_global option (minimum identity of 97%) contained in the open source program VSEARCH49. After processing, data were normalized by rarefaction based on a minimum sample size of 23,850 reads. One hundred independent normalization runs were conducted and the average abundance for all normalization runs was used in further analyses. The biome file was imported into microbiome analyst (http://www.microbiomeanalyst.ca/) for further analysis. Unique reads and those that were not present in at least twenty percent of the samples were excluded. Measures of alpha (Chao1 estimates at OTU level, Shannon diversity index at species level) and beta diversity (Bray-Curtis distances at species level).

Statistics

Data are expressed as mean ± SEM. Statistical analysis was performed using two-way ANOVA (Genotype by Transplant) and one-way ANOVA with Tukey's post hoc test (SPSS for Windows, release 11.5.0; SPSS, Chicago, IL). A mixed model ANOVA (within factor, dose; between factor, recipient group) was used for EDD and EID dose response curves. When a significant main effect was observed, Tukey's post-hoc test was performed to determine specific pairwise differences. A p-value of <0.05 was considered statistically significant. Correlation analysis between outcome measures was performed using GraphPad Prism (La Jolla, CA).

Results

Prior to transplant, we first sought to confirm that the Con and Ob donor mice displayed differences in gut permeability and vascular function. *In vivo* assessment of gut permeability

showed greater gut permeability in Ob mice (Figure 4.1A). Also, as expected, Ob mice had higher aortic pulse wave velocity (aPWV)(Figure 4.1B) and impaired ACh-mediated endothelium-dependent dilation (EDD)(Figure 4.1C) compared to Con mice, whereas endothelium-independent dilation (EID) was not significantly different between groups (Figure 4.1D). Cecal content was collected from this subset of Ob (with established vascular dysfunction) and Con mice (with normal vascular function) and pooled to create homogenous donor samples. Following suppression of endogenous microbiota with antibiotics, transplants were performed for eight weeks via oral gavage of donor samples. Once the transplants were completed, bacterial DNA was extracted from fecal pellets for 16S sequencing.

Following microbiota transplant, we examined whether recipient genotype and microbiota transplant differentially affected indices of alpha and beta diversity. Chao1 richness, a statistical estimate of the number of organisms present in a sample, was significantly lower in the two Ob groups compared to Con+Con, whereas the Con+Ob group was not significantly different from either Con+Con or Ob+Ob (Figure 4.2A). The same pattern was observed for Shannon diversity, which accounts for both richness and evenness the microbial populations (Figure 4.2B). NMDS analysis showed that microbiota samples from recipient mice tended to cluster based on donor type (Figure 4.2C), indicating that our transplantation paradigm was generally successful.

Next, we determined the effect of microbiota transplant on fecal microbiota composition. At the phyla level, the only significant differences were observed in relative abundance of Verrucomicrobioa, which was reduced in all groups compared to Con+Con (Figure 4.3A). The percent abundance decreased from 10.2% in Con+Con to 5.7% in Con+Ob ($p=0.028$), and was nearly absent in Ob+Con (0.3%, $p<0.001$ vs Con+Con) and Ob+Ob (0.3%, $p<0.001$ vs Con+Con). Although the abundance of Bacteriodetes was lower in Ob mice (main effect of genotype, $p=0.011$), there was no significant effect of transplant. A similar effect of genotype

was observed at the class level. That is, Ob mice displayed reduced abundance of Clostridia (main effect of genotype, p=0.001), with no significant effect of transplant (Figure 4.3B). Further analysis revealed that the abundance of several bacterial species were altered by microbiota transplant, while others remained unaffected (Figure 4.3C-E). Of note, the abundance of *Akkermansia muciniphila*, the primary taxa within the phyla Verrucomicrobia, was significantly reduced in Con+Ob mice compared to Con+Con (Figure 4.3C). *A. muciniphila* abundance was further reduced in each of the Ob groups compared to the two Con groups. Levels of *Bacteroides spp.* were also strongly affected based on transplant type, with significantly higher levels present in Con+Ob and Ob+Ob mice compared to Con+Con and Ob+Con mice (Figure 4.3D). Lastly, *Oscillospira spp.* was not significantly altered by transplant type and showed reduced expression in both Ob groups compared with Con mice (Figure 3E).

To determine the effect of transplant on the production of microbial fermentation products and gut permeability. We observed that mice receiving the Con microbiota displayed significantly higher levels of all three short-chain fatty acids (SCFA): acetate (main effect of transplant, p=0.008), propionate (main effect of transplant, p<0.001) and butyrate (main effect of transplant, p<0.001)(Figure 4.4A). Specifically, the concentration of propionate and butyrate were significantly reduced in Con+Ob compared to Con+Con, while levels of these SCFA were significantly higher in Ob+Con compared to Ob+Ob. Gut permeability was increased in Con+Ob compared to Con+Con mice (Figure 4.4B). However, microbiota transplant did not alter gut permeability in Ob mice. Of note, microbiota transplants did not affect the rate of body weight gain during the transplant period in either Con or Ob mice, nor did it lead to significant differences in body composition (Table 4.1).

We next examined the effect of transplant on vascular function. We found that arterial stiffness was significantly increased in Con+Ob mice compared to Con+Con (Figure 4.5A). In contrast, transplant of the Con microbiota did not affect arterial stiffness in Ob mice (Figure

4.5A). At termination, Ob mice displayed impaired maximal ACh-mediated dilation compared to Con (main effect of genotype, p=0.008), but neither EDD nor EID were significantly altered by microbiota transplant in either Con or Ob mice (Figure 4.5B-C). Finally, correlation analysis showed a strong inverse relation between fecal *A. muciniphila* abundance and aPWV across all recipient mice (Figure 4.6).

Discussion

The primary finding of the current study was that 8 weeks transplant of Ob microbiota to Con mice promoted the development of arterial stiffness, without affecting endothelial function. The increase in arterial stiffness was associated with augmented gut permeability, reduced fecal abundance of *A. muciniphila* and cecal SCFA levels, and was independent of body weight and other morphological characteristics. In contrast to our hypothesis, transplant of Con microbiota to Ob mice was insufficient to attenuate either arterial stiffness or endothelial dysfunction. The lack of change observed in these Ob mice may be related to the inability of our transplant protocol to meaningfully impact the gut microbial composition and/or reduce gut permeability. Finally, arterial stiffness was inversely correlated with *A. muciniphila* abundance, suggesting a potential role for this bacterium in modulating arterial stiffness. Collectively, our results provide new evidence that gut dysbiosis may represent a novel cause of obesity-related arterial stiffness; and extend the growing body of literature supporting a role of the gut microbiota in regulating cardiovascular function and disease (8).

The gut microbiome is emerging as a key regulator of host physiological function, and adverse changes in the composition of the intestinal microbiota, termed dysbiosis, have been observed in obesity (16, 81). In the gastrointestinal tract of both humans and mice is host to bacterial species belong primarily to two principal phyla, the Firmicutes and Bacteroidetes (80, 139). Early work by Ley et al., found that *ob/ob* mice display significant reductions in Bacteroidetes compared to their lean wild-type littermates, and this observation was later

confirmed in obese humans (80, 81). In line with these findings, our analysis also found a lower relative abundance of Bacteroidetes in Ob mice; however, we did not observe significant differences between Con or Ob groups following microbiota transplant.

A more intriguing finding in the present study was that transplant of the Ob microbiota to Con mice caused a significant reduction in the abundance of *A. muciniphila.* Our finding that Ob mice display near complete absence of *A. muciniphila* agrees with previous work in *ob/ob* mice (34). Interestingly, *A. muciniphila* and *Oscillospira*, which we also found to be higher in mice receiving Con microbiota, have been observed to be in higher prevalence in cardiometabolically healthy and normal weight individuals (30), and the relative abundance of *A. muciniphila* is positively correlated with measures of intestinal health (88). Recent studies have begun to reveal the mechanisms by which *A. muciniphila* can regulate barrier function. Chelakkot et al., found that *A. muciniphila*-derived extracellular vesicles reduce gut permeability in part by increasing expression of the tight junction occludin (24). Plovier et al., demonstrated that Amuc_1100, a specific protein isolated from the outer membrane of *A. muciniphila*, can improve the gut barrier through a mechanism involving Toll-like receptor 2 (109). Thus, the increased gut permeability observed in Con mice receiving Ob microbiota may be explained, at least in part, by the reduced abundance of *A. muciniphila*.

Certain gut bacteria are capable of fermenting dietary fibers to produce short chain fatty acids (SCFAs). The most abundant SCFAs are acetate, propionate and butyrate; and these molecules have wide-ranging effects on host physiology. For example, butyrate serves as the preferred fuel source for colonic epithelial cells and promotes epithelial barrier function (65). SCFAs produced by the gut microbiota also regulate blood pressure via olfactory receptor and G protein-coupled receptor (GPCR) signaling (110). Natarajan et al., reported that SCFAs acetate and propionate induce endothelium-dependent, but eNOS-independent, dilation in isolated resistance arteries from mice (96). These researchers also found that mice lacking a

SCFA receptor, Gpr41, display isolated systolic hypertension and elevated aortic pulse wave velocity, associated with increased aortic thickening (96), suggesting that low SCFA levels may contribute to arterial stiffening through an increase in vascular tone. Therefore, in the present study, a reduction in SCFA levels in Con mice receiving Ob microbiota may represent a contributing factor to the increase in gut permeability and arterial stiffness in these mice. It is intriguing that while we observed higher concentrations of propionate and butyrate in Ob mice receiving Con microbiota, these changes were not associated with changes to gut permeability and arterial stiffness. In the future, it will be important to determine if responses to SCFAs are in any way altered in *ob/ob* mice.

Murine models of obesity, including the *ob/ob* strain, have been used extensively to study the role of the dysbiosis in obesity-related diseases independent of dietary composition (16, 19, 34-36, 80). Although no studies to date have investigated the role of the gut microbiota in the development of vascular dysfunction in leptin-deficient Ob mice, this rodent model has been widely used to study mechanisms underlying obesity-related vascular dysfunction (25, 104, 134, 153). However, the use of these animals is not without its limitations. For example, leptin has been shown to regulate aortic compliance independent of its effects on body weight (128). Amar et al., also discovered a role for leptin in regulating the translocation of intestinal bacteria (2). These researchers showed that Ob mice display higher levels of total bacterial DNA in the blood compared to wild-type mice, and that treatment with a leptin-producing probiotic reduced bacterial adherence and translocation.

We, and others, have previously used murine models of high-fat diet-induced obesity to study mechanisms related to the development of vascular dysfunction. Although the use of Ob mice in the present study was chosen to eliminate the confounding effect of diet on the gut microbiota, the use of this genetic obesity model may have limited our ability to effectively examine the vascular effects of transplanting the Con microbiota to Ob mice. Ob mice display

marked metabolic dysfunction and inflammation in various tissues even when fed a standard maintenance diet (14, 16), and this dramatic phenotype may explain the lack of change in measures of gut permeability or vascular function in these mice. Alternatively, these null findings may be related to the inability our transplant protocol to adequately modulate the microbiota composition in Ob mice, as evidenced by persistent low abundance of *A. muciniphila* in the Ob+Con group (Figure 4.3C). To our knowledge, no previous studies to date have examined the effects of altering the gut microbiota of Ob mice via microbiota transplant, which may reflect the difficulty in successfully conducting these experiments. Alternative methods of modulating the gut microbiota, including prebiotic and/or probiotic supplementation, may represent a more prudent strategy to affect intestinal and systemic physiology in these mice, and should be considered in future studies.

Regarding endothelial function, the duration of microbiota transplant (8 weeks) may have been insufficient time for the development or attenuation of dysbiosis-related endothelial dysfunction. Western diet (WD) feeding has been shown to shift microbiota composition within 24 hours (124, 140), however it may take up to 5 months for WD feeding to induce vascular dysfunction (7). Therefore, it is possible that microbiota transplant would elicit changes to endothelial function if performed over a longer period.

In conclusion, the present work confirms previous research linking obesity to gut dysbiosis, and is the first to demonstrate that obesity-related changes to the gut microbiota can elicit arterial stiffening in lean wild-type mice. The data also provide insight into the potential upstream mediators of arterial stiffening, and identify *A. muciniphila* as a potential therapeutic target in the treatment and prevention of obesity-related vascular dysfunction.

Figures

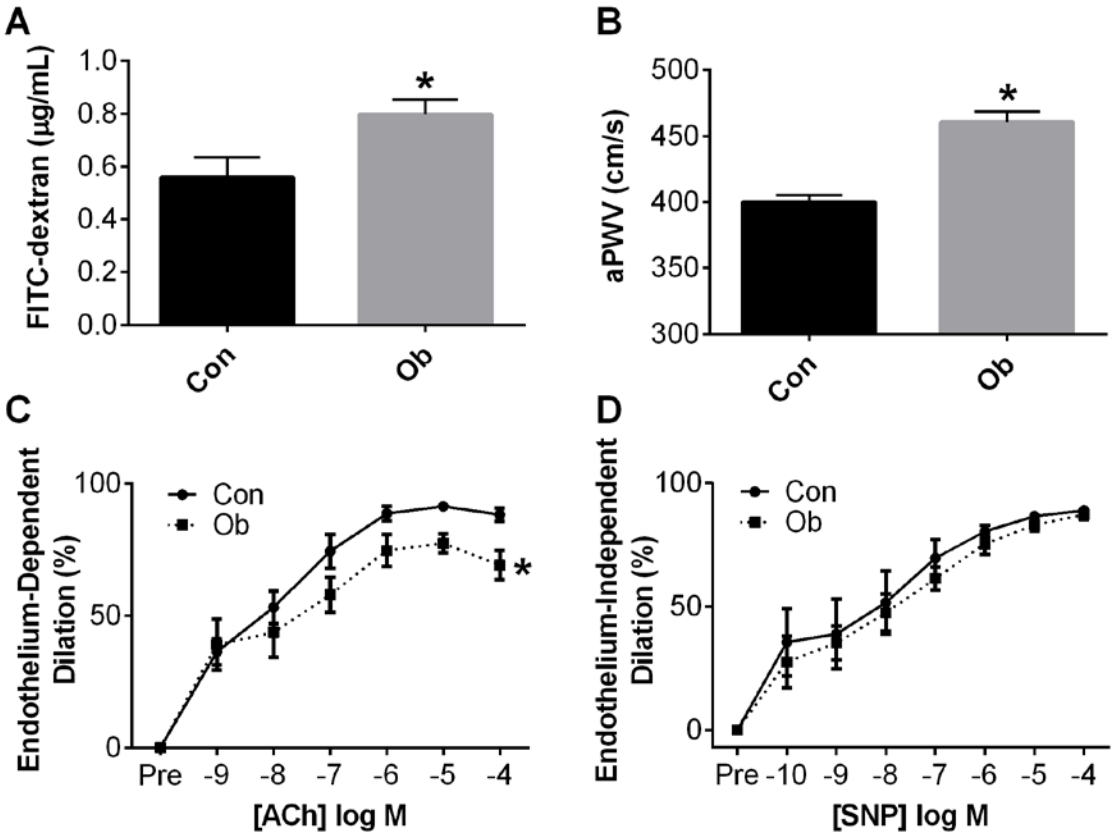

Figure 4.1. Assessment of vascular function and gut permeability in obese and wild-type donor mice. Gut permeability was assessed as plasma FITC-dextran concentration four hours after oral administration in *ob/ob* (Ob) and wild-type (Con) mice (A). Arterial stiffness was measured by *in vivo* aortic pulse wave velocity (aPWV) (B). Endothelium-dependent dilation (EDD) to acetylcholine (ACh) and endothelium-dependent dilation (EID) to sodium nitroprusside (SNP) were determined in mesenteric arteries (C-D). Data are expressed as mean ± SEM; n = 5-6/group. Statistical analysis was performed using two-tailed students t-test. *P < 0.05 vs Con.

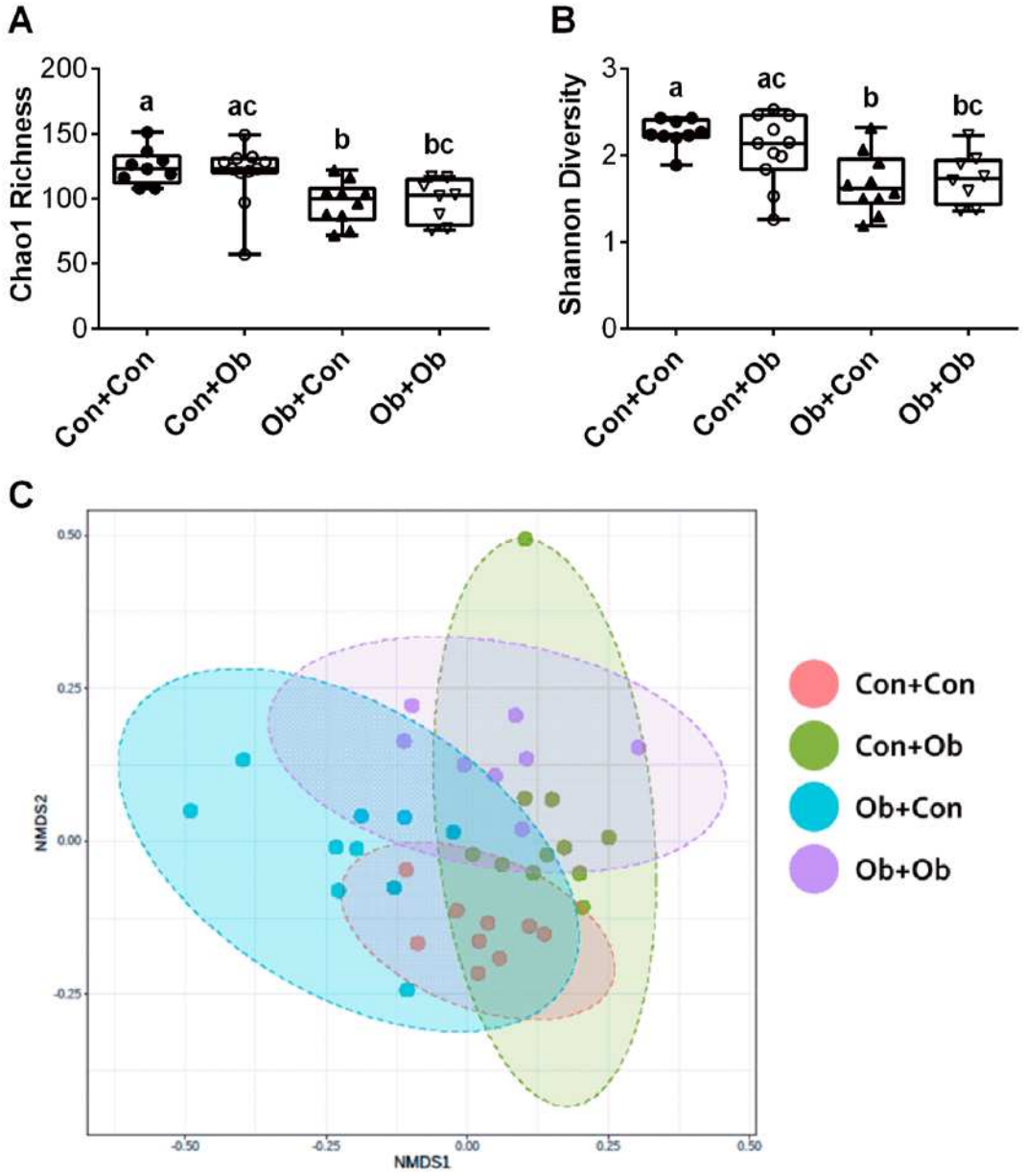

Figure 4.2. Effects of microbiota transplant on measures of microbial diversity. Alpha diversity was determined by Chao1 richness (A) and Shannon diversity (B). NMDS biplot of mouse fecal microbial communities colored by recipient group. Distance measurements between samples (beta diversity) was determined at the species level by Bray-Curtis index (C). Data are expressed as mean ± SEM; n = 9-11/group. Statistical analysis was performed using one-way ANOVA with Tukey's post hoc test. Data with different superscript letters are significantly different ($P < 0.05$).

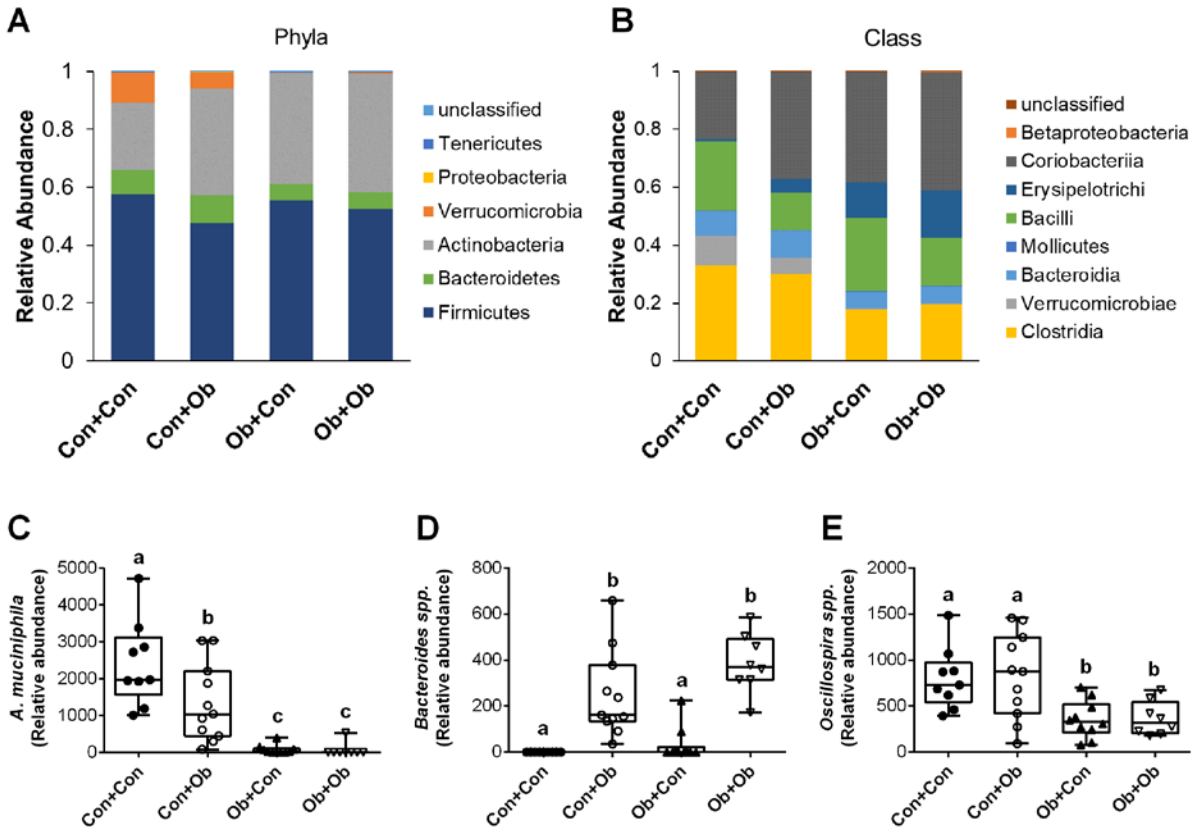

Figure 4.3. Effects of microbiota transplant on bacterial abundance at the phyla, class and species level. Relative abundance of fecal bacteria at the phyla (A) and class (B) levels. Relative abundance of fecal *Akkermansia muciniphila* (C), *Bacteroides spp.* (D), and *Oscillospira spp.* (E). Data are expressed as mean ± SEM; n = 9-11/group. Statistical analysis was performed using one-way ANOVA with Tukey's post hoc test. Data with different superscript letters are significantly different ($P < 0.05$).

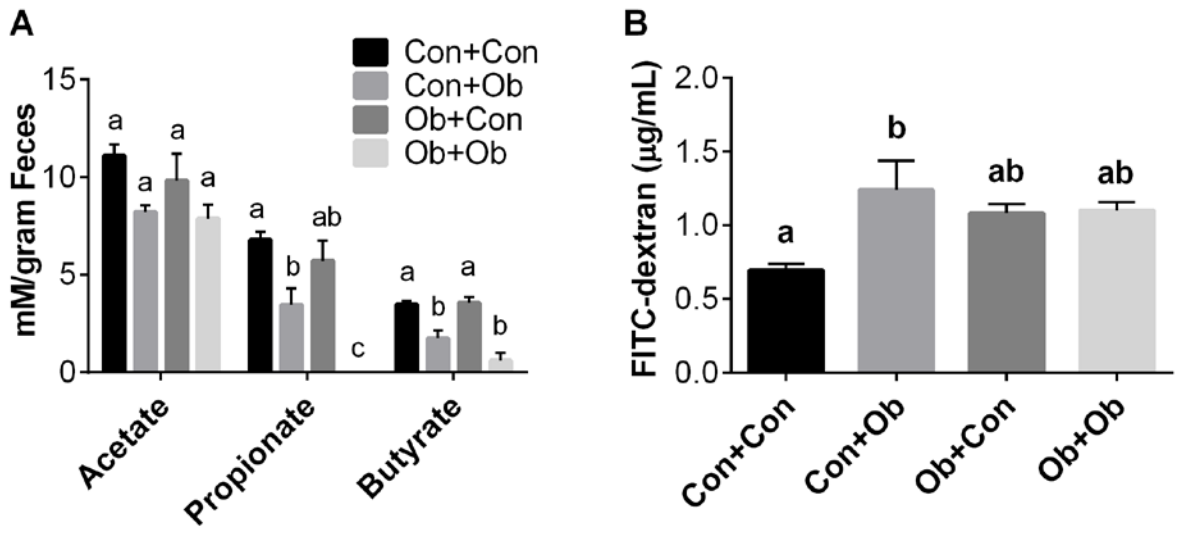

Figure 4.4. Effects of microbiota transplant on SCFA production and gut permeability. Short-chain fatty acid (SCFA) concentrations were determined in cecal content (A). Gut permeability was assessed as plasma FITC-dextran concentration four hours after administration (B). Data are expressed as mean ± SEM; n = 9-11/group. Statistical analysis was performed using one-way ANOVA with Tukey's post hoc test. Data with different superscript letters are significantly different ($P < 0.05$).

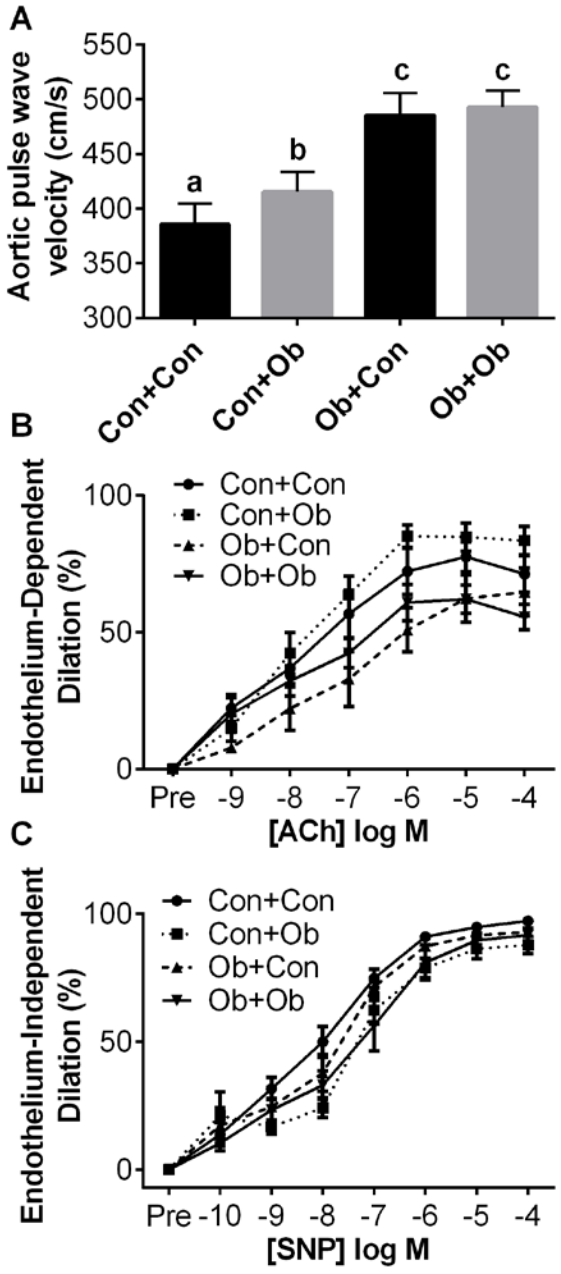

Figure 4.5. Effects of microbiota transplant on arterial stiffness and endothelial dysfunction. Arterial stiffness was measured by *in vivo* aortic pulse wave velocity (aPWV) (A). Endothelium-dependent dilation (EDD) to acetylcholine (ACh) and endothelium-dependent dilation (EID) to sodium nitroprusside (SNP) were determined in mesenteric arteries (B-C). Data are expressed as mean ± SEM; n = 9-11/group. Statistical analysis was performed using one-way ANOVA with Tukey's post hoc test. Data with different superscript letters are significantly different ($P < 0.05$).

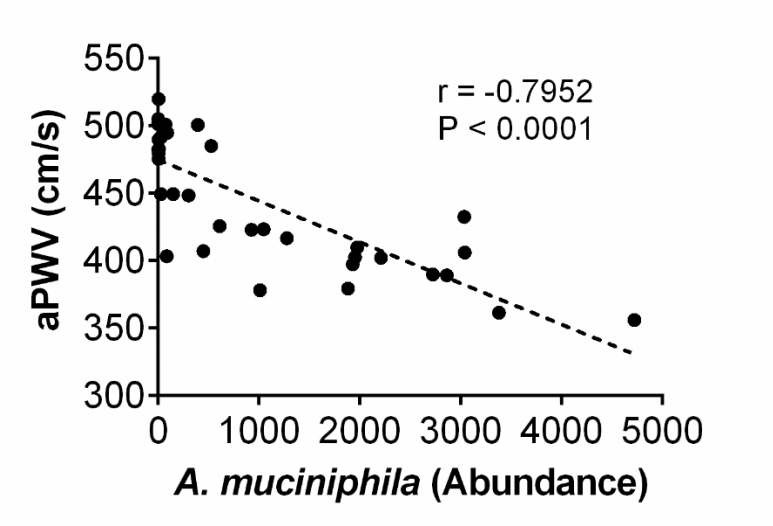

Figure 4.6. Correlation of *Akkermansia muciniphila* abundance with arterial stiffness. Correlation of fecal *A. muciniphila* abundance with aortic pulse wave velocity (aPWV) among all recipient mice. Pearson correlation coefficient (r) and P value are indicated in figure; n = 7-12/group.

Tables

Table 4.1. Characteristics of recipient mice following microbiota transplant.

	Con+Con	Con+Ob	Ob+Con	Ob+Ob
Body weight (g)	29.9 ± 1.0^{a}	29.7 ± 0.6^{a}	56.4 ± 1.0^{b}	62.1 ± 1.8^{c}
Change in body weight (g)	3.1 ± 0.4^{a}	2.0 ± 0.5^{a}	7.7 ± 0.7^{b}	8.8 ± 0.8^{b}
Epididymal fat mass (mg)	835.5 ± 99.0^{a}	730.4 ± 77.4^{a}	1928.2 ± 127.7^{b}	2302.7 ± 211.1^{b}
Subcutaneous fat mass (mg)	428.9 ± 60.1^{a}	464.6 ± 49.1^{a}	5063.2 ± 281.2^{b}	6033.2 ± 536.7^{b}
Mesenteric fat mass (mg)	344.9 ± 43.2^{a}	348.3 ± 36.1^{a}	1149.1 ± 57.9^{b}	1038.0 ± 142.1^{b}
PVAT mass (mg)	23.3 ± 2.7^{a}	29.4 ± 3.2^{a}	140.5 ± 12.1^{b}	164.3 ± 10.4^{b}
Spleen mass (mg)	101.7 ± 8.6^{a}	92.4 ± 6.0^{a}	187.5 ± 32.8^{b}	212.2 ± 14.4^{b}
Cecum mass (mg)	298.4 ± 13.9^{a}	328.3 ± 19.4^{ab}	403.0 ± 36.1^{b}	377.2 ± 35.1^{ab}
Colon length (cm)	6.4 ± 0.3^{a}	6.5 ± 0.1^{a}	8.1 ± 0.3^{b}	8.4 ± 0.3^{b}

PVAT = perivascular adipose tissue. Data are expressed as mean ± SEM; n = 7-11/group. Statistical analysis was performed using one-way ANOVA with Tukey's post hoc test. Data with different superscript letters are significantly different (P < 0.05).

CHAPTER 5: SUMMARY AND FUTURE DIRECTIONS

The epidemics of obesity and type 2 diabetes in the U.S. and worldwide contribute significantly to the rising prevalence of cardiovascular diseases (CVD). Vascular dysfunction, which manifests clinically as arterial stiffness and endothelial dysfunction, represents an important link between these metabolic diseases and cardiovascular events and mortality. The pathophysiological changes that lead to arterial stiffness and endothelial dysfunction likely stem from a combination of adverse cellular processes, including endoplasmic reticulum (ER) stress, inflammation, and oxidative stress. Therefore, it is crucial to identify the underlying causes of these cellular stresses, and examine the potential efficacy of treatments targeted at improving vascular function in obesity and type 2 diabetes.

The studies conducted as part of this dissertation research examined 1) the role of ER stress in diabetes-related vascular dysfunction and 2) the role of the gut microbiota in obesity-related vascular dysfunction. First, we tested the hypothesis that inhibition of ER stress with the chemical chaperone TUDCA would improve vascular function in type 2 diabetic mice. We found that both acute (*ex vivo*) and chronic (*in vivo*) administration of TUDCA improved mesenteric artery endothelial function. Chronic TUDCA administration also reduced arterial stiffness and was associated with reduced expression of ER stress markers in the aorta and surrounding perivascular adipose tissue. Building on this, and previously published work from our laboratory in nondiabetic obese humans (58), an upcoming study will examine the effect of TUDCA administration on endothelial function in obese humans.

Next, we tested the hypothesis that antibiotic-mediated suppression of the gut microbiota would attenuate vascular dysfunction in Western diet (WD)-induced obese mice. Seven months of WD feeding caused gut dysbiosis, increased arterial stiffness and endothelial dysfunction, and promoted inflammation within the circulation and vasculature. Antibiotic treatment

successfully suppressed the gut microbiota and reversed WD-induced arterial stiffness and endothelial dysfunction. These improvements were accompanied by reductions in inflammation, and independent from changes in body weight and glucose tolerance. Interestingly, impairments in vascular function were strongly correlated with reductions in *Bifidobacterium spp*., and this finding served as the basis for an ongoing follow-up study testing whether supplementation with *Bifidobacterium spp*. can prevent the development of WD-induced arterial stiffness and endothelial dysfunction.

Lastly, utilizing microbiota transplants, we tested the hypotheses that 1) the gut microbiota of leptin-deficient, *ob/ob* (Ob) mice contribute to the development of vascular dysfunction and 2) the gut microbiota of wild-type (Con) mice can attenuate vascular dysfunction in Ob mice. We found that microbiota transplant caused significant changes to several bacterial species and altered microbial short-chain fatty acid production in recipient mice. Transplant of the Ob microbiota to Con mice caused an increase in gut permeability and increased arterial stiffness, whereas transplant of a Con microbiota to Ob mice was not able to reduce gut permeability or arterial stiffness. Endothelial function was not affected by microbiota transplant in either Con or Ob mice. Ongoing analyses are being conducted to examine the potential mechanisms underlying the changes in barrier function and arterial stiffness. Future studies will translate these findings to human obesity and examine whether vascular phenotypes (normal or impaired vascular function) can be recapitulated in germ-free mice following microbiota transplant from lean and obese subjects.

REFERENCES

1. Adnan S, Nelson JW, Ajami NJ, Venna VR, Petrosino JF, Bryan RM, Jr., and Durgan DJ. Alterations in the gut microbiota can elicit hypertension in rats. *Physiol Genomics* 49: 96-104, 2017.

2. Amar J, Chabo C, Waget A, Klopp P, Vachoux C, Bermudez-Humaran LG, Smirnova N, Berge M, Sulpice T, Lahtinen S, Ouwehand A, Langella P, Rautonen N, Sansonetti PJ, and Burcelin R. Intestinal mucosal adherence and translocation of commensal bacteria at the early onset of type 2 diabetes: molecular mechanisms and probiotic treatment. *EMBO molecular medicine* 3: 559-572, 2011.

3. Amin A, Choi SK, Galan M, Kassan M, Partyka M, Kadowitz P, Henrion D, Trebak M, Belmadani S, and Matrougui K. Chronic inhibition of endoplasmic reticulum stress and inflammation prevents ischaemia-induced vascular pathology in type II diabetic mice. *J Pathol* 227: 165-174, 2012.

4. Bacchetti De Gregoris T, Aldred N, Clare AS, and Burgess JG. Improvement of phylum- and class-specific primers for real-time PCR quantification of bacterial taxa. *J Microbiol Methods* 86: 351-356, 2011.

5. Battson ML, Lee DM, and Gentile CL. Endoplasmic Reticulum Stress and the Development of Endothelial Dysfunction. *Am J Physiol Heart Circ Physiol* ajpheart 00437 02016, 2016.

6. Battson ML, Lee DM, Jarrell DK, Hou S, Ecton KE, Phan AB, and Gentile CL. Tauroursodeoxycholic Acid Reduces Arterial Stiffness and Improves Endothelial Dysfunction in Type 2 Diabetic Mice. *J Vasc Res* 54: 280-287, 2017.

7. Battson ML, Lee DM, Jarrell DK, Hou S, Ecton KE, Weir TL, and Gentile CL. Suppression of gut dysbiosis reverses western diet-induced vascular dysfunction. *Am J Physiol Endocrinol Metab* 2017.

8. Battson ML, Lee DM, Weir TL, and Gentile CL. The gut microbiota as a novel regulator of cardiovascular function and disease. *J Nutr Biochem* 2017.

9. Belin de Chantemele EJ, and Stepp DW. Influence of obesity and metabolic dysfunction on the endothelial control in the coronary circulation. *J Mol Cell Cardiol* 52: 840-847, 2012.

10. Boutagy NE, McMillan RP, Frisard MI, and Hulver MW. Metabolic endotoxemia with obesity: Is it real and is it relevant? *Biochimie* 2015.

11. Brasier AR. The nuclear factor-kappaB-interleukin-6 signalling pathway mediating vascular inflammation. *Cardiovasc Res* 86: 211-218, 2010.

12. Briones AM, Nguyen Dinh Cat A, Callera GE, Yogi A, Burger D, He Y, Correa JW, Gagnon AM, Gomez-Sanchez CE, Gomez-Sanchez EP, Sorisky A, Ooi TC, Ruzicka M, Burns KD, and Touyz RM. Adipocytes produce aldosterone through calcineurin-dependent signaling pathways: implications in diabetes mellitus-associated obesity and vascular dysfunction. *Hypertension* 59: 1069-1078, 2012.

13. Brown JM, and Hazen SL. The gut microbial endocrine organ: bacterially derived signals driving cardiometabolic diseases. *Annu Rev Med* 66: 343-359, 2015.

14. Brun P, Castagliuolo I, Di Leo V, Buda A, Pinzani M, Palu G, and Martines D. Increased intestinal permeability in obese mice: new evidence in the pathogenesis of nonalcoholic steatohepatitis. *Am J Physiol Gastrointest Liver Physiol* 292: G518-525, 2007.

15. Cani PD, Amar J, Iglesias MA, Poggi M, Knauf C, Bastelica D, Neyrinck AM, Fava F, Tuohy KM, Chabo C, Waget A, Delmee E, Cousin B, Sulpice T, Chamontin B, Ferrieres J, Tanti JF, Gibson GR, Casteilla L, Delzenne NM, Alessi MC, and Burcelin R. Metabolic endotoxemia initiates obesity and insulin resistance. *Diabetes* 56: 1761-1772, 2007.

16. Cani PD, Bibiloni R, Knauf C, Waget A, Neyrinck AM, Delzenne NM, and Burcelin R. Changes in gut microbiota control metabolic endotoxemia-induced inflammation in high-fat diet-induced obesity and diabetes in mice. *Diabetes* 57: 1470-1481, 2008.

17. Cani PD, Neyrinck AM, Fava F, Knauf C, Burcelin RG, Tuohy KM, Gibson GR, and Delzenne NM. Selective increases of bifidobacteria in gut microflora improve high-fat-diet-induced diabetes in mice through a mechanism associated with endotoxaemia. *Diabetologia* 50: 2374-2383, 2007.

18. Cani PD, Osto M, Geurts L, and Everard A. Involvement of gut microbiota in the development of low-grade inflammation and type 2 diabetes associated with obesity. *Gut Microbes* 3: 279-288, 2012.

19. Cani PD, Possemiers S, Van de Wiele T, Guiot Y, Everard A, Rottier O, Geurts L, Naslain D, Neyrinck A, Lambert DM, Muccioli GG, and Delzenne NM. Changes in gut microbiota control inflammation in obese mice through a mechanism involving GLP-2-driven improvement of gut permeability. *Gut* 58: 1091-1103, 2009.

20. Cao SS, and Kaufman RJ. Endoplasmic reticulum stress and oxidative stress in cell fate decision and human disease. *Antioxid Redox Signal* 21: 396-413, 2014.

21. Carvalho BM, Guadagnini D, Tsukumo DML, Schenka AA, Latuf-Filho P, Vassallo J, Dias JC, Kubota LT, Carvalheira JBC, and Saad MJA. Modulation of gut microbiota by antibiotics improves insulin signalling in high-fat fed mice. *Diabetologia* 55: 2823-2834, 2012.

22. Catry E, Bindels LB, Tailleux A, Lestavel S, Neyrinck AM, Goossens JF, Lobysheva I, Plovier H, Essaghir A, Demoulin JB, Bouzin C, Pachikian BD, Cani PD, Staels B, Dessy C, and Delzenne NM. Targeting the gut microbiota with inulin-type fructans: preclinical demonstration of a novel approach in the management of endothelial dysfunction. *Gut* 2017.

23. Cheang WS, Tian XY, Wong WT, Lau CW, Lee SS, Chen ZY, Yao X, Wang N, and Huang Y. Metformin protects endothelial function in diet-induced obese mice by inhibition of endoplasmic reticulum stress through 5' adenosine monophosphate-activated protein kinase-

peroxisome proliferator-activated receptor delta pathway. *Arterioscler Thromb Vasc Biol* 34: 830-836, 2014.

24. Chelakkot C, Choi Y, Kim DK, Park HT, Ghim J, Kwon Y, Jeon J, Kim MS, Jee YK, Gho YS, Park HS, Kim YK, and Ryu SH. Akkermansia muciniphila-derived extracellular vesicles influence gut permeability through the regulation of tight junctions. *Exp Mol Med* 50: e450, 2018.

25. Chen JY, Tsai PJ, Tai HC, Tsai RL, Chang YT, Wang MC, Chiou YW, Yeh ML, Tang MJ, Lam CF, Shiesh SC, Li YH, Tsai WC, Chou CH, Lin LJ, Wu HL, and Tsai YS. Increased aortic stiffness and attenuated lysyl oxidase activity in obesity. *Arterioscler Thromb Vasc Biol* 33: 839-846, 2013.

26. Choi SK, Lim M, Yeon SI, and Lee YH. Inhibition of endoplasmic reticulum stress improves coronary artery function in type 2 diabetic mice. *Exp Physiol* 101: 768-777, 2016.

27. Cnop M, Foufelle F, and Velloso LA. Endoplasmic reticulum stress, obesity and diabetes. *Trends Mol Med* 18: 59-68, 2012.

28. Cruickshank K, Riste L, Anderson SG, Wright JS, Dunn G, and Gosling RG. Aortic pulse-wave velocity and its relationship to mortality in diabetes and glucose intolerance: an integrated index of vascular function? *Circulation* 106: 2085-2090, 2002.

29. Dandekar A, Mendez R, and Zhang K. Cross talk between ER stress, oxidative stress, and inflammation in health and disease. *Methods in molecular biology* 1292: 205-214, 2015.

30. de la Cuesta-Zuluaga J, Corrales-Agudelo V, Carmona JA, Abad JM, and Escobar JS. Body size phenotypes comprehensively assess cardiometabolic risk and refine the association between obesity and gut microbiota. *Int J Obes (Lond)* 2017.

31. Donato AJ, Henson GD, Morgan RG, Enz RA, Walker AE, and Lesniewski LA. TNF-alpha impairs endothelial function in adipose tissue resistance arteries of mice with diet-induced obesity. *Am J Physiol Heart Circ Physiol* 303: H672-679, 2012.

32. Du B, Ouyang A, Eng JS, and Fleenor BS. Aortic perivascular adipose-derived interleukin-6 contributes to arterial stiffness in low-density lipoprotein receptor deficient mice. *Am J Physiol Heart Circ Physiol* 308: H1382-1390, 2015.

33. Durgan DJ, Ganesh BP, Cope JL, Ajami NJ, Phillips SC, Petrosino JF, Hollister EB, and Bryan RM, Jr. Role of the Gut Microbiome in Obstructive Sleep Apnea-Induced Hypertension. *Hypertension* 67: 469-474, 2016.

34. Ellekilde M, Selfjord E, Larsen CS, Jakesevic M, Rune I, Tranberg B, Vogensen FK, Nielsen DS, Bahl MI, Licht TR, Hansen AK, and Hansen CH. Transfer of gut microbiota from lean and obese mice to antibiotic-treated mice. *Sci Rep* 4: 5922, 2014.

35. Everard A, Belzer C, Geurts L, Ouwerkerk JP, Druart C, Bindels LB, Guiot Y, Derrien M, Muccioli GG, Delzenne NM, de Vos WM, and Cani PD. Cross-talk between Akkermansia muciniphila and intestinal epithelium controls diet-induced obesity. *Proc Natl Acad Sci U S A* 110: 9066-9071, 2013.

36. Everard A, Lazarevic V, Derrien M, Girard M, Muccioli GG, Neyrinck AM, Possemiers S, Van Holle A, Francois P, de Vos WM, Delzenne NM, Schrenzel J, and Cani PD. Responses of gut microbiota and glucose and lipid metabolism to prebiotics in genetic obese and diet-induced leptin-resistant mice. *Diabetes* 60: 2775-2786, 2011.

37. Finkelstein EA, Khavjou OA, Thompson H, Trogdon JG, Pan L, Sherry B, and Dietz W. Obesity and severe obesity forecasts through 2030. *American journal of preventive medicine* 42: 563-570, 2012.

38. Fleenor BS, Eng JS, Sindler AL, Pham BT, Kloor JD, and Seals DR. Superoxide signaling in perivascular adipose tissue promotes age-related artery stiffness. *Aging Cell* 13: 576-578, 2014.

39. Franconi F, Seghieri G, Canu S, Straface E, Campesi I, and Malorni W. Are the available experimental models of type 2 diabetes appropriate for a gender perspective? *Pharmacological research* 57: 6-18, 2008.

40. Fry JL, Al Sayah L, Weisbrod RM, Van Roy I, Weng X, Cohen RA, Bachschmid MM, and Seta F. Vascular Smooth Muscle Sirtuin-1 Protects Against Diet-Induced Aortic Stiffness. *Hypertension* 68: 775-784, 2016.

41. Galili O, Versari D, Sattler KJ, Olson ML, Mannheim D, McConnell JP, Chade AR, Lerman LO, and Lerman A. Early experimental obesity is associated with coronary endothelial dysfunction and oxidative stress. *Am J Physiol Heart Circ Physiol* 292: H904-911, 2007.

42. Ganne S, and Winer N. Vascular compliance in the cardiometabolic syndrome. *J Cardiometab Syndr* 3: 35-39, 2008.

43. Ganz ML, Wintfeld N, Li Q, Alas V, Langer J, and Hammer M. The association of body mass index with the risk of type 2 diabetes: a case-control study nested in an electronic health records system in the United States. *Diabetol Metab Syndr* 6: 50, 2014.

44. Gentile CL, and Pagliassotti MJ. The endoplasmic reticulum as a potential therapeutic target in nonalcoholic fatty liver disease. *Current opinion in investigational drugs* 9: 1084-1088, 2008.

45. Gil-Ortega M, Martin-Ramos M, Arribas SM, Gonzalez MC, Aranguez I, Ruiz-Gayo M, Somoza B, and Fernandez-Alfonso MS. Arterial stiffness is associated with adipokine dysregulation in non-hypertensive obese mice. *Vascul Pharmacol* 77: 38-47, 2016.

46. Goldin A, Beckman JA, Schmidt AM, and Creager MA. Advanced glycation end products: sparking the development of diabetic vascular injury. *Circulation* 114: 597-605, 2006.

47. Gregory JC, Buffa JA, Org E, Wang Z, Levison BS, Zhu W, Wagner MA, Bennett BJ, Li L, DiDonato JA, Lusis AJ, and Hazen SL. Transmission of atherosclerosis susceptibility with gut microbial transplantation. *J Biol Chem* 290: 5647-5660, 2015.

48. Gustafsson BE, and Maunsbach AB. Ultrastructure of the enlargec cecum in germfree rats. *Z Zellforsch Mikrosk Anat* 120: 555-578, 1971.

49. Haffner SM, Lehto S, Ronnemaa T, Pyorala K, and Laakso M. Mortality from coronary heart disease in subjects with type 2 diabetes and in nondiabetic subjects with and without prior myocardial infarction. *N Engl J Med* 339: 229-234, 1998.

50. Hales CM, Carroll MD, Fryar CD, and Ogden C. Prevalence of obesity among adults and youth: United States, 2015–2016. Hyattsville, MD: National Center for Health Statistics, 2017.

51. Hirota M, Kitagaki M, Itagaki H, and Aiba S. Quantitative measurement of spliced XBP1 mRNA as an indicator of endoplasmic reticulum stress. *J Toxicol Sci* 31: 149-156, 2006.

52. Hotamisligil GS. Endoplasmic reticulum stress and the inflammatory basis of metabolic disease. *Cell* 140: 900-917, 2010.

53. Huang Cao ZF, Stoffel E, and Cohen P. Role of Perivascular Adipose Tissue in Vascular Physiology and Pathology. *Hypertension* 69: 770-777, 2017.

54. Iantorno M, Campia U, Di Daniele N, Nistico S, Forleo GB, Cardillo C, and Tesauro M. Obesity, inflammation and endothelial dysfunction. *J Biol Regul Homeost Agents* 28: 169-176, 2014.

55. International R. Cardiovascular Disease: A Costly Burden for America American Heart Association: 2017.

56. Jain S, Khera R, Corrales-Medina VF, Townsend RR, and Chirinos JA. "Inflammation and arterial stiffness in humans". *Atherosclerosis* 237: 381-390, 2014.

57. Jia G, Aroor AR, DeMarco VG, Martinez-Lemus LA, Meininger GA, and Sowers JR. Vascular stiffness in insulin resistance and obesity. *Frontiers in physiology* 6: 231, 2015.

58. Kaplon RE, Chung E, Reese L, Cox-York K, Seals DR, and Gentile CL. Activation of the unfolded protein response in vascular endothelial cells of nondiabetic obese adults. *J Clin Endocrinol Metab* 98: E1505-1509, 2013.

59. Karbach SH, Schonfelder T, Brandao I, Wilms E, Hormann N, Jackel S, Schuler R, Finger S, Knorr M, Lagrange J, Brandt M, Waisman A, Kossmann S, Schafer K, Munzel T,

Reinhardt C, and Wenzel P. Gut Microbiota Promote Angiotensin II-Induced Arterial Hypertension and Vascular Dysfunction. *Journal of the American Heart Association* 5: 2016.

60. Karima Ait Aissa MK, Mohamed Trebak, Souad Belmadani and Khalid Matrougui. Role of endoplasmic reticulum stress and thrombosis in type 2 diabetes-induced vascular dysfunction. *The FASEB Journal* 29: 2015.

61. Karlsson CL, Onnerfalt J, Xu J, Molin G, Ahrne S, and Thorngren-Jerneck K. The microbiota of the gut in preschool children with normal and excessive body weight. *Obesity (Silver Spring)* 20: 2257-2261, 2012.

62. Karlsson F, Tremaroli V, Nielsen J, and Backhed F. Assessing the human gut microbiota in metabolic diseases. *Diabetes* 62: 3341-3349, 2013.

63. Kassan M, Vikram A, Li Q, Kim YR, Kumar S, Gabani M, Liu J, Jacobs JS, and Irani K. MicroRNA-204 promotes vascular endoplasmic reticulum stress and endothelial dysfunction by targeting Sirtuin1. *Sci Rep* 7: 9308, 2017.

64. Katz PS, Trask AJ, Souza-Smith FM, Hutchinson KR, Galantowicz ML, Lord KC, Stewart JA, Jr., Cismowski MJ, Varner KJ, and Lucchesi PA. Coronary arterioles in type 2 diabetic (db/db) mice undergo a distinct pattern of remodeling associated with decreased vessel stiffness. *Basic research in cardiology* 106: 1123-1134, 2011.

65. Kelly CJ, Zheng L, Campbell EL, Saeedi B, Scholz CC, Bayless AJ, Wilson KE, Glover LE, Kominsky DJ, Magnuson A, Weir TL, Ehrentraut SF, Pickel C, Kuhn KA, Lanis JM, Nguyen V, Taylor CT, and Colgan SP. Crosstalk between Microbiota-Derived Short-Chain Fatty Acids and Intestinal Epithelial HIF Augments Tissue Barrier Function. *Cell host & microbe* 17: 662-671, 2015.

66. Ketonen J, Shi J, Martonen E, and Mervaala E. Periadventitial adipose tissue promotes endothelial dysfunction via oxidative stress in diet-induced obese C57Bl/6 mice. *Circ J* 74: 1479-1487, 2010.

67. Kim F, Pham M, Luttrell I, Bannerman DD, Tupper J, Thaler J, Hawn TR, Raines EW, and Schwartz MW. Toll-like receptor-4 mediates vascular inflammation and insulin resistance in diet-induced obesity. *Circ Res* 100: 1589-1596, 2007.

68. Kim JA, Jang HJ, and Hwang DH. Toll-like receptor 4-induced endoplasmic reticulum stress contributes to impairment of vasodilator action of insulin. *Am J Physiol Endocrinol Metab* 309: E767-776, 2015.

69. Kinlay S, Michel T, and Leopold JA. The Future of Vascular Biology and Medicine. *Circulation* 133: 2603-2609, 2016.

70. Kobayasi R, Akamine EH, Davel AP, Rodrigues MA, Carvalho CR, and Rossoni LV. Oxidative stress and inflammatory mediators contribute to endothelial dysfunction in high-fat diet-induced obesity in mice. *J Hypertens* 28: 2111-2119, 2010.

71. Koeth RA, Wang Z, Levison BS, Buffa JA, Org E, Sheehy BT, Britt EB, Fu X, Wu Y, Li L, Smith JD, DiDonato JA, Chen J, Li H, Wu GD, Lewis JD, Warrier M, Brown JM, Krauss RM, Tang WH, Bushman FD, Lusis AJ, and Hazen SL. Intestinal microbiota metabolism of L-carnitine, a nutrient in red meat, promotes atherosclerosis. *Nat Med* 19: 576-585, 2013.

72. Konishi T, Idezuki Y, Kobayashi H, Shimada K, Iwai S, Yamaguchi K, and Shinagawa N. Oral vancomycin hydrochloride therapy for postoperative methicillin-cephem-resistant Staphylococcus aureus enteritis. *Surgery today* 27: 826-832, 1997.

73. Kunun CM. Absorption of Orally Administered Neomycin and Kanamycin — With Special Reference to Patients with Severe Hepatic and Renal Disease. *NEJM* 262: 380-385, 1960.

74. Laugerette F, Alligier M, Bastard JP, Drai J, Chanseaume E, Lambert-Porcheron S, Laville M, Morio B, Vidal H, and Michalski MC. Overfeeding increases postprandial endotoxemia in men: Inflammatory outcome may depend on LPS transporters LBP and sCD14. *Molecular nutrition & food research* 58: 1513-1518, 2014.

75. Laugerette F, Furet JP, Debard C, Daira P, Loizon E, Geloen A, Soulage CO, Simonet C, Lefils-Lacourtablaise J, Bernoud-Hubac N, Bodennec J, Peretti N, Vidal H, and Michalski

MC. Oil composition of high-fat diet affects metabolic inflammation differently in connection with endotoxin receptors in mice. *Am J Physiol Endocrinol Metab* 302: E374-386, 2012.

76. Laukens D, Brinkman BM, Raes J, De Vos M, and Vandenabeele P. Heterogeneity of the gut microbiome in mice: guidelines for optimizing experimental design. *FEMS Microbiol Rev* 40: 117-132, 2016.

77. Lee DM, Battson ML, Jarrell DK, Cox-York K, Foster MT, Weir TL, and Gentile CL. Fuzhuan tea reverses arterial stiffening after modest weight gain in mice. *Nutrition* 2016.

78. Lee KS, Kim J, Kwak SN, Lee KS, Lee DK, Ha KS, Won MH, Jeoung D, Lee H, Kwon YG, and Kim YM. Functional role of NF-kappaB in expression of human endothelial nitric oxide synthase. *Biochem Biophys Res Commun* 448: 101-107, 2014.

79. Lesniewski LA, Durrant JR, Connell ML, Folian BJ, Donato AJ, and Seals DR. Salicylate treatment improves age-associated vascular endothelial dysfunction: potential role of nuclear factor kappaB and forkhead Box O phosphorylation. *J Gerontol A Biol Sci Med Sci* 66: 409-418, 2011.

80. Ley RE, Backhed F, Turnbaugh P, Lozupone CA, Knight RD, and Gordon JI. Obesity alters gut microbial ecology. *Proc Natl Acad Sci U S A* 102: 11070-11075, 2005.

81. Ley RE, Turnbaugh PJ, Klein S, and Gordon JI. Microbial ecology: human gut microbes associated with obesity. *Nature* 444: 1022-1023, 2006.

82. Li J, Lin S, Vanhoutte PM, Woo CW, and Xu A. Akkermansia Muciniphila Protects Against Atherosclerosis by Preventing Metabolic Endotoxemia-Induced Inflammation in Apoe-/- Mice. *Circulation* 133: 2434-2446, 2016.

83. Li L, Sun Q, Li Y, Yang Y, Yang Y, Chang T, Man M, and Zheng L. Overexpression of SIRT1 Induced by Resveratrol and Inhibitor of miR-204 Suppresses Activation and Proliferation of Microglia. *Journal of molecular neuroscience : MN* 56: 858-867, 2015.

84. Li M, Liang P, Li Z, Wang Y, Zhang G, Gao H, Wen S, and Tang L. Fecal microbiota transplantation and bacterial consortium transplantation have comparable effects on the re-

establishment of mucosal barrier function in mice with intestinal dysbiosis. *Front Microbiol* 6: 692, 2015.

85. Li Volti G, Salomone S, Sorrenti V, Mangiameli A, Urso V, Siarkos I, Galvano F, and Salamone F. Effect of silibinin on endothelial dysfunction and ADMA levels in obese diabetic mice. *Cardiovasc Diabetol* 10: 62, 2011.

86. Liang CF, Liu JT, Wang Y, Xu A, and Vanhoutte PM. Toll-like receptor 4 mutation protects obese mice against endothelial dysfunction by decreasing NADPH oxidase isoforms 1 and 4. *Arterioscler Thromb Vasc Biol* 33: 777-784, 2013.

87. Lindstrom P. The physiology of obese-hyperglycemic mice [ob/ob mice]. *ScientificWorldJournal* 7: 666-685, 2007.

88. Liu TW, Cephas KD, Holscher HD, Kerr KR, Mangian HF, Tappenden KA, and Swanson KS. Nondigestible Fructans Alter Gastrointestinal Barrier Function, Gene Expression, Histomorphology, and the Microbiota Profiles of Diet-Induced Obese C57BL/6J Mice. *J Nutr* 146: 949-956, 2016.

89. Lorber D. Importance of cardiovascular disease risk management in patients with type 2 diabetes mellitus. *Diabetes, metabolic syndrome and obesity : targets and therapy* 7: 169-183, 2014.

90. Manter DK, Korsa M, Tebbe C, and Delgado JA. myPhyloDB: a local web server for the storage and analysis of metagenomic data. *Database (Oxford)* 2016: 2016.

91. Mell B, Jala VR, Mathew AV, Byun J, Waghulde H, Zhang Y, Haribabu B, Vijay-Kumar M, Pennathur S, and Joe B. Evidence for a link between gut microbiota and hypertension in the Dahl rat. *Physiol Genomics* 47: 187-197, 2015.

92. Mitchell GF, Hwang SJ, Vasan RS, Larson MG, Pencina MJ, Hamburg NM, Vita JA, Levy D, and Benjamin EJ. Arterial stiffness and cardiovascular events: the Framingham Heart Study. *Circulation* 121: 505-511, 2010.

93. Mozaffarian D, Benjamin EJ, Go AS, Arnett DK, Blaha MJ, Cushman M, de Ferranti S, Despres JP, Fullerton HJ, Howard VJ, Huffman MD, Judd SE, Kissela BM, Lackland DT, Lichtman JH, Lisabeth LD, Liu S, Mackey RH, Matchar DB, McGuire DK, Mohler ER, 3rd, Moy CS, Muntner P, Mussolino ME, Nasir K, Neumar RW, Nichol G, Palaniappan L, Pandey DK, Reeves MJ, Rodriguez CJ, Sorlie PD, Stein J, Towfighi A, Turan TN, Virani SS, Willey JZ, Woo D, Yeh RW, Turner MB, American Heart Association Statistics C, and Stroke Statistics S. Heart disease and stroke statistics--2015 update: a report from the American Heart Association. *Circulation* 131: e29-322, 2015.

94. Munford RS. Endotoxemia-menace, marker, or mistake? *J Leukoc Biol* 100: 687-698, 2016.

95. Murakami M, Tognini P, Liu Y, Eckel-Mahan KL, Baldi P, and Sassone-Corsi P. Gut microbiota directs PPARgamma-driven reprogramming of the liver circadian clock by nutritional challenge. *EMBO Rep* 17: 1292-1303, 2016.

96. Natarajan N, Hori D, Flavahan S, Steppan J, Flavahan NA, Berkowitz DE, and Pluznick JL. Microbial short chain fatty acid metabolites lower blood pressure via endothelial G-protein coupled receptor 41. *Physiol Genomics* physiolgenomics 00089 02016, 2016.

97. Ndumele CE, Matsushita K, Lazo M, Bello N, Blumenthal RS, Gerstenblith G, Nambi V, Ballantyne CM, Solomon SD, Selvin E, Folsom AR, and Coresh J. Obesity and Subtypes of Incident Cardiovascular Disease. *Journal of the American Heart Association* 5: 2016.

98. Neves AL, Coelho J, Couto L, Leite-Moreira A, and Roncon-Albuquerque R, Jr. Metabolic endotoxemia: a molecular link between obesity and cardiovascular risk. *J Mol Endocrinol* 51: R51-64, 2013.

99. Nosalski R, and Guzik TJ. Perivascular adipose tissue inflammation in vascular disease. *Br J Pharmacol* 2017.

100. Ouyang A, Garner TB, and Fleenor BS. Hesperidin reverses perivascular adipose-mediated aortic stiffness with aging. *Exp Gerontol* 97: 68-72, 2017.

101. Ozcan U, Cao Q, Yilmaz E, Lee AH, Iwakoshi NN, Ozdelen E, Tuncman G, Gorgun C, Glimcher LH, and Hotamisligil GS. Endoplasmic reticulum stress links obesity, insulin action, and type 2 diabetes. *Science* 306: 457-461, 2004.

102. Ozcan U, Yilmaz E, Ozcan L, Furuhashi M, Vaillancourt E, Smith RO, Gorgun CZ, and Hotamisligil GS. Chemical chaperones reduce ER stress and restore glucose homeostasis in a mouse model of type 2 diabetes. *Science* 313: 1137-1140, 2006.

103. Palombo C, and Kozakova M. Arterial stiffness, atherosclerosis and cardiovascular risk: Pathophysiologic mechanisms and emerging clinical indications. *Vascul Pharmacol* 77: 1-7, 2016.

104. Paneni F, Costantino S, and Cosentino F. p66(Shc)-induced redox changes drive endothelial insulin resistance. *Atherosclerosis* 236: 426-429, 2014.

105. Park KH, and Park WJ. Endothelial Dysfunction: Clinical Implications in Cardiovascular Disease and Therapeutic Approaches. *J Korean Med Sci* 30: 1213-1225, 2015.

106. Perticone F, Ceravolo R, Pujia A, Ventura G, Iacopino S, Scozzafava A, Ferraro A, Chello M, Mastroroberto P, Verdecchia P, and Schillaci G. Prognostic significance of endothelial dysfunction in hypertensive patients. *Circulation* 104: 191-196, 2001.

107. Pfaffenbach KT, Gentile CL, Nivala AM, Wang D, Wei Y, and Pagliassotti MJ. Linking endoplasmic reticulum stress to cell death in hepatocytes: roles of C/EBP homologous protein and chemical chaperones in palmitate-mediated cell death. *Am J Physiol Endocrinol Metab* 298: E1027-1035, 2010.

108. Pierce GL, Lesniewski LA, Lawson BR, Beske SD, and Seals DR. Nuclear factor-{kappa}B activation contributes to vascular endothelial dysfunction via oxidative stress in overweight/obese middle-aged and older humans. *Circulation* 119: 1284-1292, 2009.

109. Plovier H, Everard A, Druart C, Depommier C, Van Hul M, Geurts L, Chilloux J, Ottman N, Duparc T, Lichtenstein L, Myridakis A, Delzenne NM, Klievink J, Bhattacharjee A, van der Ark KC, Aalvink S, Martinez LO, Dumas ME, Maiter D, Loumaye A, Hermans MP, Thissen JP,

Belzer C, de Vos WM, and Cani PD. A purified membrane protein from Akkermansia muciniphila or the pasteurized bacterium improves metabolism in obese and diabetic mice. *Nat Med* 23: 107-113, 2017.

110. Pluznick JL, Protzko RJ, Gevorgyan H, Peterlin Z, Sipos A, Han J, Brunet I, Wan LX, Rey F, Wang T, Firestein SJ, Yanagisawa M, Gordon JI, Eichmann A, Peti-Peterdi J, and Caplan MJ. Olfactory receptor responding to gut microbiota-derived signals plays a role in renin secretion and blood pressure regulation. *Proc Natl Acad Sci U S A* 110: 4410-4415, 2013.

111. Prevention CfDCa. National Diabetes Statistics Report, 2017 Atlanta, GA: Centers for Disease Control and Prevention, U.S. Dept of Health and Human Services, 2017.

112. R D, V P, M D, V M, I N, E P, K A, D G, and S G. Obesity-Relationship with Vascular Dysfunction. *Advances in Obesity, Weight Management & Control* 1: 5, 2014.

113. Rajpal DK, Klein JL, Mayhew D, Boucheron J, Spivak AT, Kumar V, Ingraham K, Paulik M, Chen L, Van Horn S, Thomas E, Sathe G, Livi GP, Holmes DJ, and Brown JR. Selective Spectrum Antibiotic Modulation of the Gut Microbiome in Obesity and Diabetes Rodent Models. *PloS one* 10: e0145499, 2015.

114. Rakoff-Nahoum S, Paglino J, Eslami-Varzaneh F, Edberg S, and Medzhitov R. Recognition of commensal microflora by toll-like receptors is required for intestinal homeostasis. *Cell* 118: 229-241, 2004.

115. Rao S, Kupfer Y, Pagala M, Chapnick E, and Tessler S. Systemic absorption of oral vancomycin in patients with Clostridium difficile infection. *Scandinavian journal of infectious diseases* 43: 386-388, 2011.

116. Reikvam DH, Erofeev A, Sandvik A, Grcic V, Jahnsen FL, Gaustad P, McCoy KD, Macpherson AJ, Meza-Zepeda LA, and Johansen FE. Depletion of murine intestinal microbiota: effects on gut mucosa and epithelial gene expression. *PloS one* 6: e17996, 2011.

117. Reil JC, Hohl M, Reil GH, Granzier HL, Kratz MT, Kazakov A, Fries P, Muller A, Lenski M, Custodis F, Graber S, Frohlig G, Steendijk P, Neuberger HR, and Bohm M. Heart rate

reduction by If-inhibition improves vascular stiffness and left ventricular systolic and diastolic function in a mouse model of heart failure with preserved ejection fraction. *Eur Heart J* 34: 2839-2849, 2013.

118. Santacruz A, Collado MC, Garcia-Valdes L, Segura MT, Martin-Lagos JA, Anjos T, Marti-Romero M, Lopez RM, Florido J, Campoy C, and Sanz Y. Gut microbiota composition is associated with body weight, weight gain and biochemical parameters in pregnant women. *Br J Nutr* 104: 83-92, 2010.

119. Savage DC, and Dubos R. Alterations in the mouse cecum and its flora produced by antibacterial drugs. *J Exp Med* 128: 97-110, 1968.

120. Schinzari F, Iantorno M, Campia U, Mores N, Rovella V, Tesauro M, Di Daniele N, and Cardillo C. Vasodilator responses and endothelin-dependent vasoconstriction in metabolically healthy obesity and the metabolic syndrome. *Am J Physiol Endocrinol Metab* 309: E787-792, 2015.

121. Schloss PD, Westcott SL, Ryabin T, Hall JR, Hartmann M, Hollister EB, Lesniewski RA, Oakley BB, Parks DH, Robinson CJ, Sahl JW, Stres B, Thallinger GG, Van Horn DJ, and Weber CF. Introducing mothur: open-source, platform-independent, community-supported software for describing and comparing microbial communities. *Appl Environ Microbiol* 75: 7537-7541, 2009.

122. Schneeberger M, Everard A, Gomez-Valades AG, Matamoros S, Ramirez S, Delzenne NM, Gomis R, Claret M, and Cani PD. Akkermansia muciniphila inversely correlates with the onset of inflammation, altered adipose tissue metabolism and metabolic disorders during obesity in mice. *Sci Rep* 5: 16643, 2015.

123. Schram MT, Henry RM, van Dijk RA, Kostense PJ, Dekker JM, Nijpels G, Heine RJ, Bouter LM, Westerhof N, and Stehouwer CD. Increased central artery stiffness in impaired glucose metabolism and type 2 diabetes: the Hoorn Study. *Hypertension* 43: 176-181, 2004.

124. Schroeder BO, Birchenough GMH, Stahlman M, Arike L, Johansson MEV, Hansson GC, and Backhed F. Bifidobacteria or Fiber Protects against Diet-Induced Microbiota-Mediated Colonic Mucus Deterioration. *Cell host & microbe* 23: 27-40 e27, 2018.

125. Seals DR, Jablonski KL, and Donato AJ. Aging and vascular endothelial function in humans. *Clin Sci (Lond)* 120: 357-375, 2011.

126. Selvin E, Parrinello CM, Sacks DB, and Coresh J. Trends in prevalence and control of diabetes in the United States, 1988-1994 and 1999-2010. *Ann Intern Med* 160: 517-525, 2014.

127. Sena CM, Pereira AM, and Seica R. Endothelial dysfunction - a major mediator of diabetic vascular disease. *Biochim Biophys Acta* 1832: 2216-2231, 2013.

128. Sikka G, Yang R, Reid S, Benjo A, Koitabashi N, Camara A, Baraban E, O'Donnell CP, Berkowitz DE, and Barouch LA. Leptin is essential in maintaining normal vascular compliance independent of body weight. *Int J Obes (Lond)* 34: 203-206, 2010.

129. Sindler AL, Cox-York K, Reese L, Bryan NS, Seals DR, and Gentile CL. Oral nitrite therapy improves vascular function in diabetic mice. *Diabetes & vascular disease research : official journal of the International Society of Diabetes and Vascular Disease* 12: 221-224, 2015.

130. Sirker A, Zhang M, and Shah AM. NADPH oxidases in cardiovascular disease: insights from in vivo models and clinical studies. *Basic research in cardiology* 106: 735-747, 2011.

131. Stapleton PA, James ME, Goodwill AG, and Frisbee JC. Obesity and vascular dysfunction. *Pathophysiology* 15: 79-89, 2008.

132. Stehouwer CD, Henry RM, and Ferreira I. Arterial stiffness in diabetes and the metabolic syndrome: a pathway to cardiovascular disease. *Diabetologia* 51: 527-539, 2008.

133. Stoll LL, Denning GM, and Weintraub NL. Endotoxin, TLR4 signaling and vascular inflammation: potential therapeutic targets in cardiovascular disease. *Curr Pharm Des* 12: 4229-4245, 2006.

134. Taguchi K, Kobayashi T, Matsumoto T, and Kamata K. Dysfunction of endothelium-dependent relaxation to insulin via PKC-mediated GRK2/Akt activation in aortas of ob/ob mice. *Am J Physiol Heart Circ Physiol* 301: H571-583, 2011.

135. Tang WH, Kitai T, and Hazen SL. Gut Microbiota in Cardiovascular Health and Disease. *Circ Res* 120: 1183-1196, 2017.

136. Tang WH, Wang Z, Levison BS, Koeth RA, Britt EB, Fu X, Wu Y, and Hazen SL. Intestinal microbial metabolism of phosphatidylcholine and cardiovascular risk. *N Engl J Med* 368: 1575-1584, 2013.

137. Taylor KS, Heneghan CJ, Farmer AJ, Fuller AM, Adler AI, Aronson JK, and Stevens RJ. All-cause and cardiovascular mortality in middle-aged people with type 2 diabetes compared with people without diabetes in a large U.K. primary care database. *Diabetes Care* 36: 2366-2371, 2013.

138. Turnbaugh PJ, Backhed F, Fulton L, and Gordon JI. Diet-induced obesity is linked to marked but reversible alterations in the mouse distal gut microbiome. *Cell host & microbe* 3: 213-223, 2008.

139. Turnbaugh PJ, Hamady M, Yatsunenko T, Cantarel BL, Duncan A, Ley RE, Sogin ML, Jones WJ, Roe BA, Affourtit JP, Egholm M, Henrissat B, Heath AC, Knight R, and Gordon JI. A core gut microbiome in obese and lean twins. *Nature* 457: 480-484, 2009.

140. Turnbaugh PJ, Ridaura VK, Faith JJ, Rey FE, Knight R, and Gordon JI. The effect of diet on the human gut microbiome: a metagenomic analysis in humanized gnotobiotic mice. *Science translational medicine* 1: 6ra14, 2009.

141. van Schadewijk A, van't Wout EF, Stolk J, and Hiemstra PS. A quantitative method for detection of spliced X-box binding protein-1 (XBP1) mRNA as a measure of endoplasmic reticulum (ER) stress. *Cell Stress Chaperones* 17: 275-279, 2012.

142. Vikram A, Kim YR, Kumar S, Li Q, Kassan M, Jacobs JS, and Irani K. Vascular microRNA-204 is remotely governed by the microbiome and impairs endothelium-dependent vasorelaxation by downregulating Sirtuin1. *Nat Commun* 7: 12565, 2016.

143. Villacorta L, and Chang L. The role of perivascular adipose tissue in vasoconstriction, arterial stiffness, and aneurysm. *Horm Mol Biol Clin Investig* 21: 137-147, 2015.

144. Wang H, Luo W, Wang J, Guo C, Wang X, Wolffe SL, Bodary PF, and Eitzman DT. Obesity-induced endothelial dysfunction is prevented by deficiency of P-selectin glycoprotein ligand-1. *Diabetes* 61: 3219-3227, 2012.

145. Wang Z, Klipfell E, Bennett BJ, Koeth R, Levison BS, Dugar B, Feldstein AE, Britt EB, Fu X, Chung YM, Wu Y, Schauer P, Smith JD, Allayee H, Tang WH, DiDonato JA, Lusis AJ, and Hazen SL. Gut flora metabolism of phosphatidylcholine promotes cardiovascular disease. *Nature* 472: 57-63, 2011.

146. Wautier JL, and Wautier MP. Blood cells and vascular cell interactions in diabetes. *Clin Hemorheol Microcirc* 25: 49-53, 2001.

147. Weijin Zhang YZ, Xiaohua Guo, Zeng Zhenhua, Jie Wu, Yanan Liu, Jing He, Ruiting Wang, Qiaobing Huang, and Zhongqing Chen. Sirt1 protects endothelial cells against LPS-induced barrier dysfunction. *Oxidative Medicine and Cellular Longevity* 2017.

148. Widlansky ME, Gokce N, Keaney JF, Jr., and Vita JA. The clinical implications of endothelial dysfunction. *J Am Coll Cardiol* 42: 1149-1160, 2003.

149. Woodman RJ, Chew GT, and Watts GF. Mechanisms, significance and treatment of vascular dysfunction in type 2 diabetes mellitus: focus on lipid-regulating therapy. *Drugs* 65: 31-74, 2005.

150. Xia N, Horke S, Habermeier A, Closs EI, Reifenberg G, Gericke A, Mikhed Y, Munzel T, Daiber A, Forstermann U, and Li H. Uncoupling of Endothelial Nitric Oxide Synthase in Perivascular Adipose Tissue of Diet-Induced Obese Mice. *Arterioscler Thromb Vasc Biol* 36: 78-85, 2016.

151. Xia N, and Li H. The role of perivascular adipose tissue in obesity-induced vascular dysfunction. *Br J Pharmacol* 174: 3425-3442, 2017.

152. Yang J, Bindels LB, Segura Munoz RR, Martinez I, Walter J, Ramer-Tait AE, and Rose DJ. Disparate Metabolic Responses in Mice Fed a High-Fat Diet Supplemented with Maize-Derived Non-Digestible Feruloylated Oligo- and Polysaccharides Are Linked to Changes in the Gut Microbiota. *PloS one* 11: e0146144, 2016.

153. Yang R, Sikka G, Larson J, Watts VL, Niu X, Ellis CL, Miller KL, Camara A, Reinke C, Savransky V, Polotsky VY, O'Donnell CP, Berkowitz DE, and Barouch LA. Restoring leptin signaling reduces hyperlipidemia and improves vascular stiffness induced by chronic intermittent hypoxia. *Am J Physiol Heart Circ Physiol* 300: H1467-1476, 2011.

154. Yang T, Santisteban MM, Rodriguez V, Li E, Ahmari N, Carvajal JM, Zadeh M, Gong M, Qi Y, Zubcevic J, Sahay B, Pepine CJ, Raizada MK, and Mohamadzadeh M. Gut dysbiosis is linked to hypertension. *Hypertension* 65: 1331-1340, 2015.

155. Zieman SJ, Melenovsky V, and Kass DA. Mechanisms, pathophysiology, and therapy of arterial stiffness. *Arterioscler Thromb Vasc Biol* 25: 932-943, 2005.